Distributed representations of prediction error signals across the cortical hierarchy are synergistic

Frank Gelens[a,b,i], Juho Äijälä[b,i], Misako Komatsu[c], Cem Uran[d,e], Michael A. Jensen[f], Kai J. Miller[f], Robin A.A. Ince[g], Martin Vinck[d,e,j], Andres Canales-Johnson[b,h,j]

[a]*Department of Psychology, University of Amsterdam, Nieuwe Achtergracht 129-B, 1018 WT, Amsterdam, The Netherlands*
[b]*Department of Psychology, University of Cambridge, CB2 3EB Cambridge, United Kingdom*
[c]*Laboratory for Adaptive Intelligence, RIKEN Brain Science Institute, Saitama 351-0198, Japan*
[d]*Ernst Strüngmann Institute (ESI) for Neuroscience in Cooperation with Max Planck Society, 60528 Frankfurt am Main, Germany*
[e]*Donders Centre for Neuroscience, Department of Neuroinformatics, Radboud University Nijmegen, 6525 Nijmegen, Netherlands*
[f]*Department of Neurosurgery, Mayo Clinic, Rochester, Minnesota 55905*
[g]*Institute of Neuroscience and Psychology, University of Glasgow, Scotland G12 8QB, United Kingdom*
[h]*Neuropsychology and Cognitive Neurosciences Research Center, Faculty of Health Sciences, Universidad Católica del Maule, 3460000 Talca, Chile*
[i]*These authors contributed equally*
[j]*Correspondence to: Andres Canales-Johnson (afc37@cam.ac.uk), Martin Vinck (martin.vinck@esi-frankfurt.de)*

Abstract

An important question concerning inter-areal communication in the cortex is whether these interactions are synergistic, i.e. convey information beyond what can be performed by isolated signals. In other words, any two signals can either share common information (redundancy) or they can encode complementary information that is only available when both signals are considered together (synergy). Here, we dissociated cortical interactions sharing common information from those encoding complementary information during prediction error processing. To this end, we computed co-information, an information-theoretical measure that distinguishes redundant from synergistic information among brain signals. We analyzed auditory and frontal electrocorticography (ECoG) signals in five common awake marmosets performing two distinct auditory oddball tasks, and investigated to what extent event-related potentials (ERP) and broadband (BB) dynamics exhibit redundancy and synergy for auditory prediction error signals. We observed multiple patterns of redundancy and synergy across the entire cortical hierarchy with distinct dynamics. The information conveyed by ERPs and BB signals was highly synergistic even at lower stages of the hierarchy in the auditory cortex, as well as between lower and higher areas in the frontal cortex. These results indicate that the distributed representations of prediction error signals across the cortical hierarchy can be highly synergistic.

INTRODUCTION

The traditional modular view of brain function is increasingly challenged by the finding that information about external stimuli and internal variables is distributed across brain areas (de Schotten and Forkel, 2022; Urai et al., 2022; Shenoy and Kao, 2021; Breakspear, 2017; Panzeri et al., 2022). When information in a complex system is carried by multiple nodes, this could imply that there is a large degree of redundancy in the information carried by the different nodes. That is, the whole is actually less than the sum of the parts. An alternative possibility, however, is that information is carried in a synergistic manner, i.e. the different nodes might carry extra information about task variables when they are combined. In other words, the whole is more than the sum of the parts (Luppi et al., 2022).

Both recent large-scale spiking and electrocorticographic (ECoG) recordings support the notion that information about task variables is widely distributed rather than highly localized (Urai et al., 2022; Steinmetz et al., 2019; Parras et al., 2017; Saleem et al., 2018; Voitov and Mrsic-Flogel, 2022). For example, in the visual domain, widespread neuronal patterns across nearly every brain region are non-selectively activated before movement onset during a visual choice task (Steinmetz et al., 2019). Similarly, distributed and reciprocally interconnected areas of the cortex maintain high-dimensional representations of working memory (Voitov and Mrsic-Flogel, 2022). In the case of multisensory integration, sound-evoked activity and its associated motor correlate can be dissociated from spiking activity in the primary visual cortex (V1) (Lohuis et al., 2022; Bimbard et al., 2023). A last example, and the one used in the current study, is the case of communication of prediction error (PE) signals. Hierarchical predictive coding theory has been proposed as a general mechanism of processing in the brain (Rao and Ballard, 1999). The communication of prediction error (PE) signals using spikes and local field potentials (LFPs) recorded from subcortical and cortical regions reveal a large-scale hierarchy PE potentials (Parras et al., 2017).

A major question is whether such distributed signals exhibit a high degree of redundancy (i.e. shared information) or a high degree of synergy (i.e. extra information) about their corresponding task variables. Electrophysiological studies have
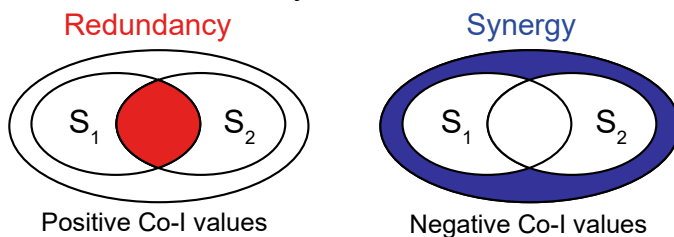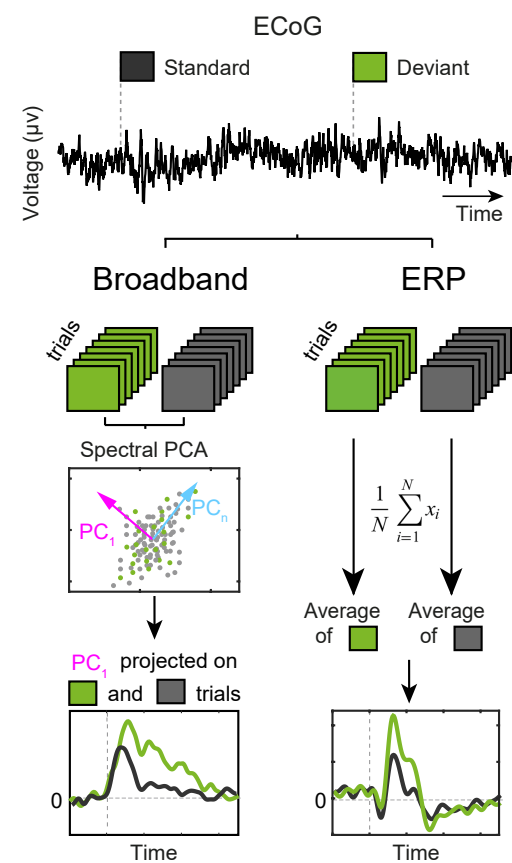
1
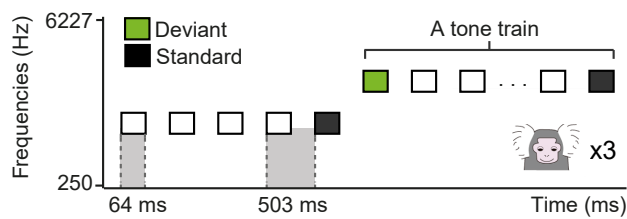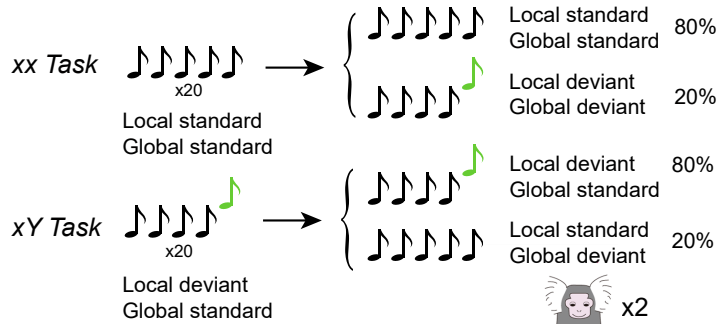
Figure 1: Experimental design, neural markers of PE, and redundancy and synergy analyses **(A)** Using a Roving oddball Task, 20 different single tones were presented in the trains of 3, 5, or 11 identical stimuli. Any two subsequent trains consisted of different tones. This way, while the adjacent standard (depicted in black) and deviant (depicted in green) tones deviated in frequency due to the transition between the trains, the two expectancy conditions were physically matched, as the first and the last tones of the same train were treated as deviant and standard tones in the analysis of the adjacent stimuli pairs. This task was performed by 3 marmosets (Fr, Kr, and Go). **(B)** Local/Global Task. On each trial, five tones of 50-ms-duration each were presented with a fixed stimulus onset asynchrony of 150 ms between sounds. The first 4 tones were identical, either low-pitched (tone A) or high-pitched (tone B), but the fifth tone could be either the same (AAAAA or BBBBB, jointly denoted by xx) or different (AAAAB or BBBBA, jointly denoted by xY). Each block started with 20 frequent series of sounds to establish global regularity before delivering the first infrequent global deviant stimulus. This task was performed by different 2 marmosets (Ji and Nr). **(C)** Neural markers of auditory prediction error. Deviant (green) and standard (black) epochs are used to compute the broadband and ERP responses. Broadband is computed by extracting by reconstructing the time series of standard and deviants with the first spectral principal component (SPCA) of the ECoG signal; ERPs are computed by averaging the raw voltage values for standard and deviant trials (see Methods). **(D)** Schematic representation of redundancy and synergy analyses computed using co-Information. Each inner oval (A1 and A2) represents the mutual information between the corresponding ECoG signals and the stimuli category (standard or deviant). The overlap between A1 and A2 represents the redundant information about the stimuli (red; left panel). The outer circle around A1 and A2 represents the synergistic information about the stimuli (blue; right panel).

shown that synergy and redundancy have functional relevance (Nigam et al., 2019; Ince et al., 2017; Park et al., 2018; Giordano et al., 2017; Luppi et al., 2022; Varley et al., 2023). For instance, laminar recordings in V1 suggest that synergistic interactions can efficiently decode visual stimuli better than redundant interactions, even in the presence of noise and overlapping receptive fields (Nigam et al., 2019). In contrast, the information processing of olfactory stimuli exhibits higher levels of redundant information across olfactory regions (Olivares et al., 2022). Here we investigate this question by using co-Information (co-I), an information theoretical metric capable of decomposing neural signals into what is informationally redundant and what is informationally synergistic between stimuli (Ince et al., 2017). Redundant information quantifies the shared information between signals, suggesting a common processing of the stimuli. Synergistic information quantifies something different: whether there is extra information only available when signals are combined, indicating that the information about the variable is in the actual relationship between the signals. We investigated synergistic and redundant interactions across ECoG signals of five common marmosets performing two types of auditory tasks. This allowed us to determine the processing of communication of prediction error information across the brain during a range of auditory deviancy effects.

RESULTS

Mutual Information reveals prediction error effects within cortical areas

To characterize the distribution of PE across multiple cortical areas, we quantified PE in each electrode of the five marmosets by contrasting deviant and standard tones (Figure 2). For each electrode, we computed Mutual Information (MI) to quantify the relationship between tone category (standard vs deviant) with their corresponding ECoG signal across trials. Within the framework of information theory, MI is a statistical quantity that measures the strength of the dependence (linear or non-linear) between two random variables. It can be also seen as the effect size, quantified in bits, for a statistical test of independence (Ince et al., 2017). Thus, for each electrode and time point, we considered ECoG signals corresponding to standard and deviant trials and utilized MI to quantify the effect size of their difference.

We have recently proposed that a suitable candidate for broadcasting unpredicted information across the cortex is the transient, aperiodic activity reflected at the level of the evoked-related potentials (ERP) and broadband power (Vinck et al., 2023). A well-studied ERP marker of auditory PE is the mismatch negativity (MMN), an ERP that peaks around 150–250 ms after the onset of an infrequent acoustic stimulus (Parras et al., 2017; Blenkmann et al., 2019; Komatsu et al., 2015; Canales-Johnson et al., 2021). A second neural marker of auditory PE is the broadband response (BB), an increase in spectral power spanning a wide range of frequencies usually above 100 Hz (Canales-Johnson et al., 2021; Jiang et al., 2022). Whereas ERPs reflect a mixture of local potentials and volume conducted potentials from distant sites, BB is an electrophysiological marker of underlying averaged spiking activity generated by the thousands of neurons that are in the immediate vicinity of the recording electrodes (Miller, 2019; Lachaux et al., 2012). MI was computed separately for the two neural markers of prediction error (i.e. ERP and BB signals).

Electrodes showing significant differences in MI over time (see METHODS) are depicted in Figure 2. In the Roving odd-ball task, ERP signals showed PE effects across multiple cortical regions not necessarily restricted to canonical auditory areas (Figure 2B). In the case of the BB signal, MI analyses revealed PE effects located predominantly in the auditory cortex of the three marmosets, as well as in a few electrodes located in the frontal cortex of marmoset Kr and Go (Figure 2A). These results agree with previous studies in different sensory modalities (Miller, 2019) showing that broadband responses are spatially localized. In the case of the Local-Global task, although the dataset for marmoset Nr and Ji contained ECoG recording only from the temporal and frontal cortices, the overall PE effects in the ERP signals were observed in a higher number o electrodes than in the BB signal (Figure 2 and Figure S9)

Co-Information reveals redundant and synergistic interactions within cortical areas

To investigate how auditory PE signals are integrated within and between the cortical hierarchy, we quantified redundant and synergistic cortical interactions using an information theoretical metric known as co-Information (co-I) (Ince et al., 2017). Co-I quantifies the type of information that interacting signals encode about a stimuli variable: positive co-I indicates redundant interactions between signals; and negative co-I accounts for synergistic interactions (Figure 1D). Redundancy implies that the signals convey the same information about PE, indicating a shared encoding of PE information across time or space from trial to trial. On the other hand, synergy implies that signals from different time points or areas convey extra information about PE only when considered together, indicating that the relationship itself contains information about PE that is not available from either of the signals alone (Figure 1D).

To quantify the dynamics of redundancy and synergy temporally and spatially, we computed the co-I within and between cortical areas (see METHODS. We analyzed ERP and BB markers of PE separately, focusing our contrasts on the electrodes that showed significant MI effects in the analyses described in Figure 2C.

Temporal synergy and redundancy

The finding that multiple recording sites encode information about PE raises the question of whether these signals convey the same or complementary PE information over time within a cortical region. Thus, we first characterized synergistic and redundant temporal interactions within ERP and BB signals. Co-I analyses revealed widespread temporal clusters of synergistic information (in blue) and redundant information (in red) across the five monkeys and across all tasks in the auditory cortex (Figure 3,4,5 A,B), and frontal cortex (Figure 3,4,5 C,D).

In the Roving task, the ERP signal in the auditory (Figure 3A) and frontal (Figure 3C) electrodes showed characteristic off-diagonal synergistic patterns, resulting from the interaction between early and late time points within the same ERP signal (e.g. Figure 3A,C; grey clusters between ~140-300 ms after tone presentation), and revealed by the single electrode contrast depicted in Figure S1. We observed significant temporal redundancy in the auditory (Figure 3B) and frontal (Figure 3D) BB signals. For auditory BB signals, the dynamics of the redundant patterns were observed along the diagonal of the co-Information chart, they were sustained over time and observed between time points around the early MI peaks (i.e., during the transient period when the effect sizes are larger between tones) (Figure 3B; grey clusters ~120-280 ms after one presentation). In the frontal electrodes, we observed significant clusters of sustained redundant interactions around later time points (Figure 3D; grey cluster around 300 ms after tone presentation).

Although PE processing has been widely studied using the Roving task (e.g. (Canales-Johnson et al., 2021)), the contribution of stimulus-specific adaptation (SSA) to the amplitude of the ERP response is usually considered a confounding factor in the isolation of PE (Parras et al., 2017). For this reason, we also investigated synergy and redundancy in a separate task capable of attenuating the effects of SSA (i.e. the Local-Global Task). In the Local task, although we observed temporal synergy in both ERP and BB signals, the off-diagonal synergistic patterns
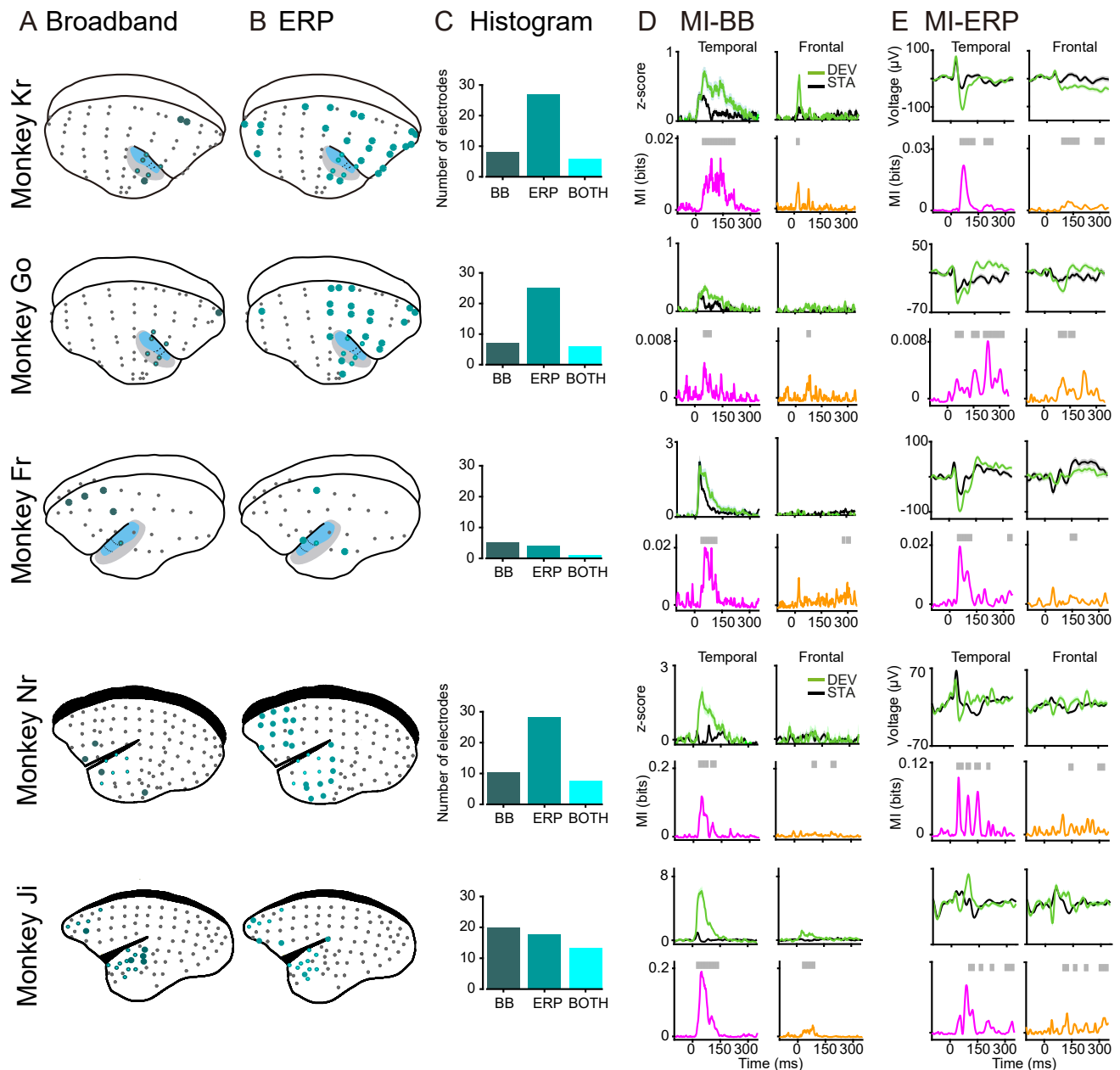
Figure 2: Broadband and ERP markers of PE across the monkey brain. Electrode locations for marmoset Kr (64 electrodes; 1st panel), Go (64 electrodes; 2nd panel), and Fr (32 electrodes; 3rd panel), Nr (96 electrodes in EcoG-array, 39 used for analyses; 4th panel) and Ji (96 electrodes in EcoG-array, 27 used for analyses; 5th panel). Electrodes showing significant PE effect after computing MI between standard and deviant trials for the **(A)** Broadband (dark green circles) and **(B)** ERP (light green circles) markers of auditory prediction error in the three monkeys. Electrodes showing significant MI for both markers are depicted in cyan. **(C)** Histogram of electrodes showing significant MI between tones for BB (left), ERP (middle), and both markers (right) for each animal. **(D)** Electrodes with the highest MI in the temporal and frontal cortex showing the BB signal for deviant and standard tones. Deviant tone (green) and standard tone (black), and the corresponding MI values in bits (effect size of the difference) for the temporal (pink trace) and frontal (orange trace) electrodes. Significant time points after a permutation test are shown as grey bars over the MI plots. **(E)** Electrodes with the highest MI in the temporal and frontal cortex showing the ERP signal for deviant and standard tones. Color codes are the same as in **C**.

characterizing the Roving task were primarily observed in the BB signal within the temporal cortex (Figure 4).

A second advantage of the Local/Global Task is the possibility of exploring a context-dependent deviancy effect observed as a violation of the overall sequence of tones (Global task; see Figure 1B, and METHODS). The context-dependant deviant has been shown to elicit neural activation in frontal re-

gions (Chao et al., 2018; Jiang et al., 2022). Interestingly, we observed temporal synergy in the Global task both within the auditory and frontal electrodes (Figure 5B,D) mainly in the BB signals, suggesting that temporally distributed information about higher-order PE is encoded primarily by firing rates.
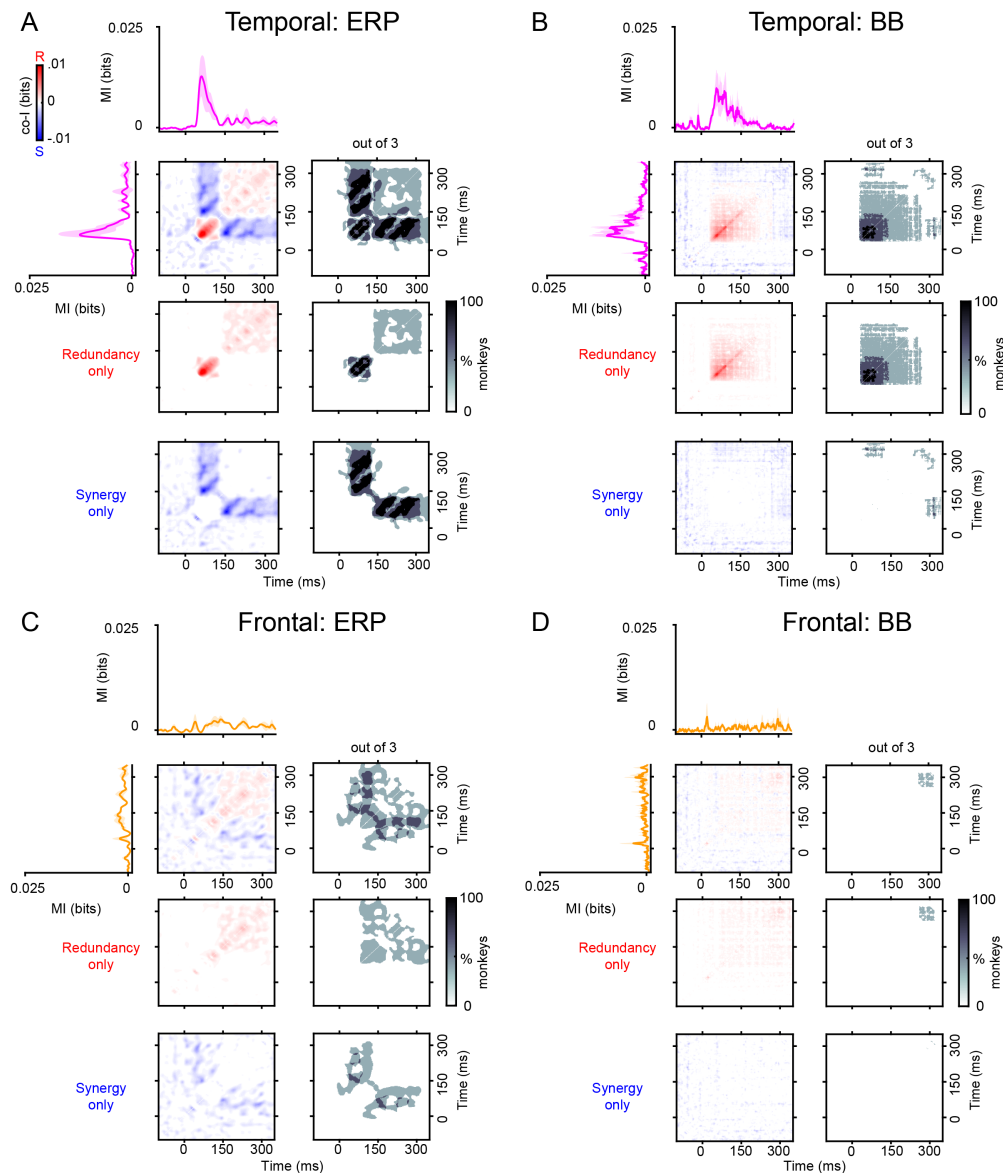
4

Figure 3: Temporal synergy and redundancy within ERP and BB signals in the auditory and frontal electrodes with the highest MI for the Roving Task. Co-information revealed synergistic and redundant temporal patterns within ERP (**A**) and BB (**B**) signals in the auditory cortex, and within ERP (**C**) and BB (**D**) signals in the frontal cortex. MI (solid traces) between standard and deviant trials for auditory (pink color) and frontal (orange color) electrodes averaged across the three monkeys. Temporal co-I was computed within the corresponding signal (ERP, BB) across time points between -100 to 350 ms after tone presentation. The average of the corresponding electrodes across monkeys is shown for the complete co-I chart (red and blue panel); for positive co-I values (redundancy only; red panel); and for negative co-I values (synergy only; blue panel). The grey panels show the proportion of monkeys showing significant co-I differences in the single electrodes analysis depicted in Figure S1.

Spatial synergy and redundancy

The finding that multiple recording sites encode information about PE raises the question of whether these regions are dynamically interacting and whether the information encoded in these interactions is carried by the ERP or BB signals. Thus, we characterized the redundancy and synergy between auditory and frontal electrodes. To this end, we computed the co-I between auditory and frontal pairs of electrodes for the same time points between signals (i.e. not across time points) to isolate

the spatial dimension of the inter-areal interactions. Spatial co-I was computed between the auditory and frontal electrodes (Figure 6) and averaged across monkeys separately for each task and signal (i.e. ERP and BB signals). In the case of the Roving task (Figure 6A-B), the results showed that only ERP signals convey spatial information about PE between areas (synergistic peak ~50-70 ms after tone presentation). Regarding the Local and Global tasks, no clear peak of synergy was observed in the ERP or BB signals (Figure 6C-F).
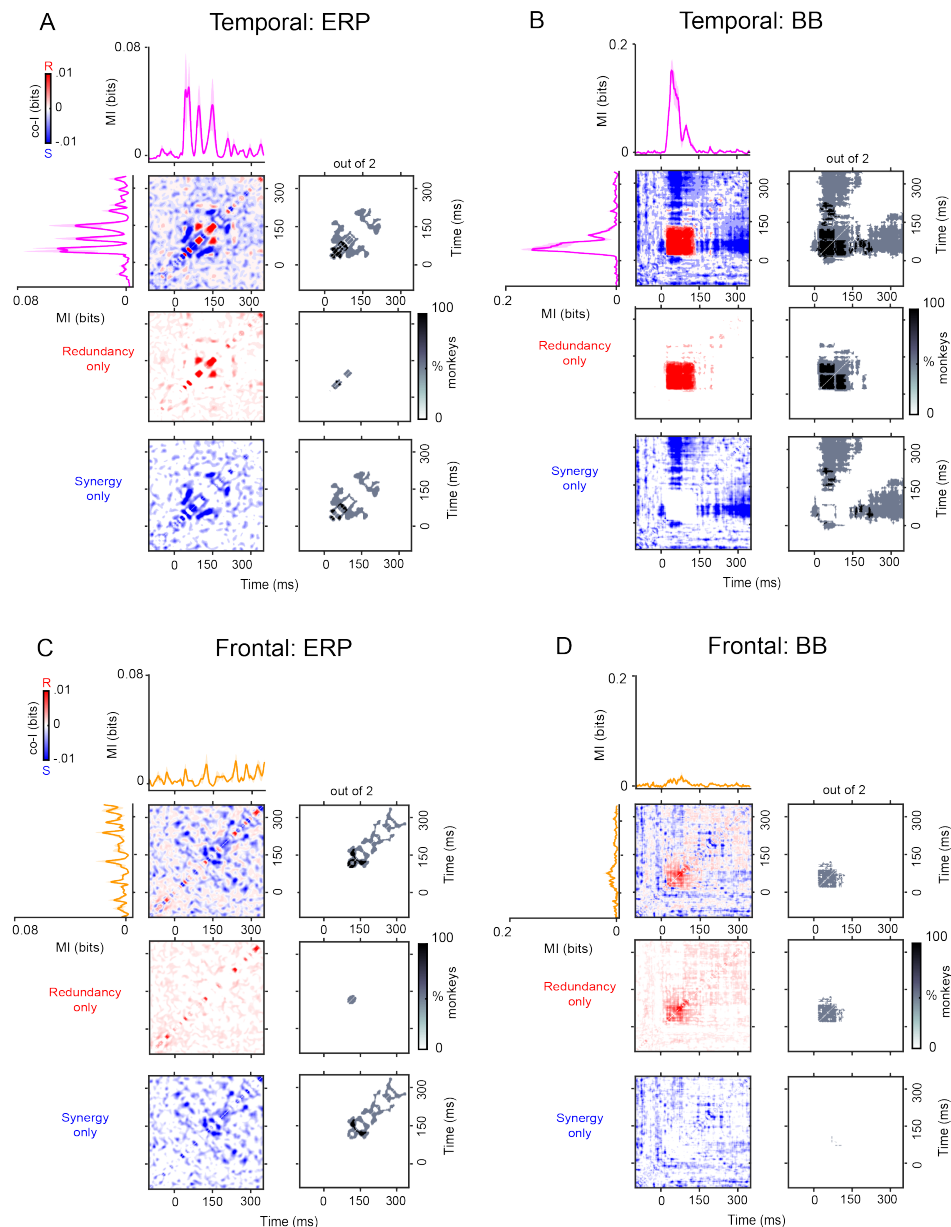
Local task

Figure 4: Temporal synergy and redundancy within ERP and BB signals in the auditory and frontal electrodes with the highest MI for the Local task. Co-information revealed synergistic and redundant temporal patterns within ERP (**A**) and BB (**B**) signals in the auditory cortex, and within ERP (**C**) and BB (**D**) signals in the frontal cortex. MI (solid traces) between standard and deviant trials for auditory (pink color) and frontal (orange color) electrodes averaged across the three monkeys. Temporal co-I was computed within the corresponding signal (ERP, BB) across time points between -100 to 350 ms after tone presentation. The average of the corresponding electrodes across monkeys is shown for the complete co-I chart (red and blue panel); for positive co-I values (redundancy only; red panel); and for negative co-I values (synergy only; blue panel). The grey panels show the proportion of monkeys showing significant co-I differences in the single electrodes analysis depicted in Figure S2.

Spatio-temporal synergy and redundancy

The observation that the Local and Global task seem to elicit lower spatial synergy than the Roving task suggests that synergistic information about PE might be encoded in more complex, spatio-temporal patterns across cortical regions depending on the task. In order to test this possibility, we computed spatio-temporal synergy and redundancy across auditory and frontal electrodes (Figure 7). As expected, the patterns of spatio-

temporal synergy in the ERP and BB signals showed more complex and heterogenous dynamics, with patterns emerging along the diagonal of the co-information chart in the Roving task (Figure 7A; e.g. ERP: blue clusters along the diagonal ~0-350 ms after tone presentation), and through off-diagonal patterns between early time points of the auditory electrodes and later time points in the frontal electrodes in the same task for both ERP and BB signals (Figure 7A,B; blue clusters between 150 ms and
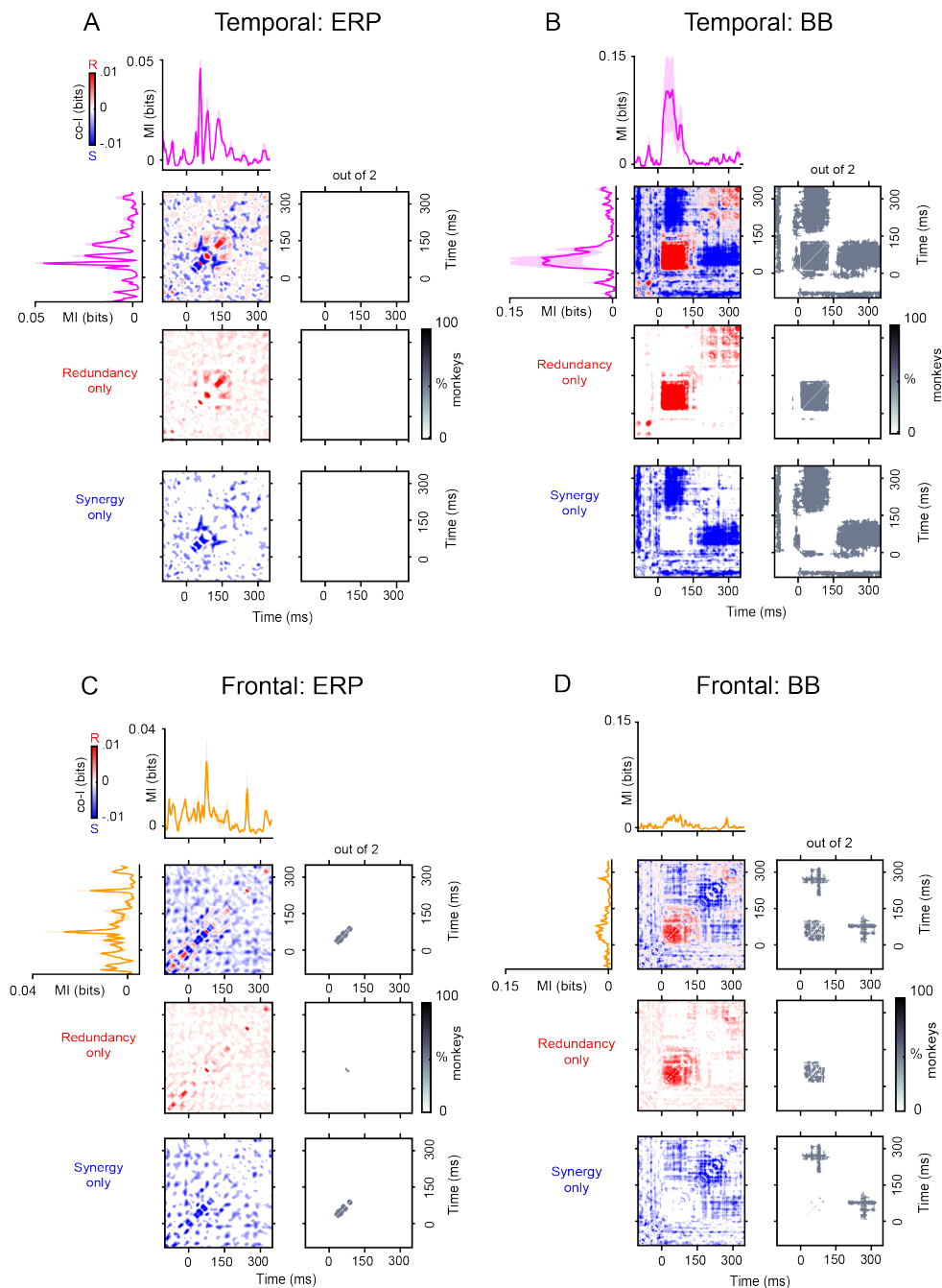
Global task

Figure 5: Temporal synergy and redundancy within ERP and BB signals in the auditory and frontal electrodes with the highest MI for the Global task. Co-information revealed synergistic and redundant temporal patterns within ERP (**A**) and BB (**B**) signals in the auditory cortex, and within ERP (**C**) and BB (**D**) signals in the frontal cortex. MI (solid traces) between standard and deviant trials for auditory (pink color) and frontal (orange color) electrodes averaged across the three monkeys. Temporal co-I was computed within the corresponding signal (ERP, BB) across time points between -100 to 350 ms after tone presentation. The average of the corresponding electrodes across monkeys is shown for the complete co-I chart (red and blue panel); for positive co-I values (redundancy only; red panel); and for negative co-I values (synergy only; blue panel). The grey panels show the proportion of monkeys showing significant co-I differences in the single electrodes analysis depicted in Figure S2.

---

350 ms after tone presentation). In the Local Task, diagonal and off-diagonal synergy was observed in both the BB-signal and the ERP (Figure 7D; e.g. BB: blue clusters between ~0-350 ms after tone presentation, C; e.g., ERP: blue clusters be-

tween ~100-250 ms after tone presentation). In contrast, for the Global task, off-diagonal synergy was mostly observed within the BB-signal (Figure 7F; e.g. BB: blue clusters between ~150-350 ms after tone presentation). On the other hand, redundancy
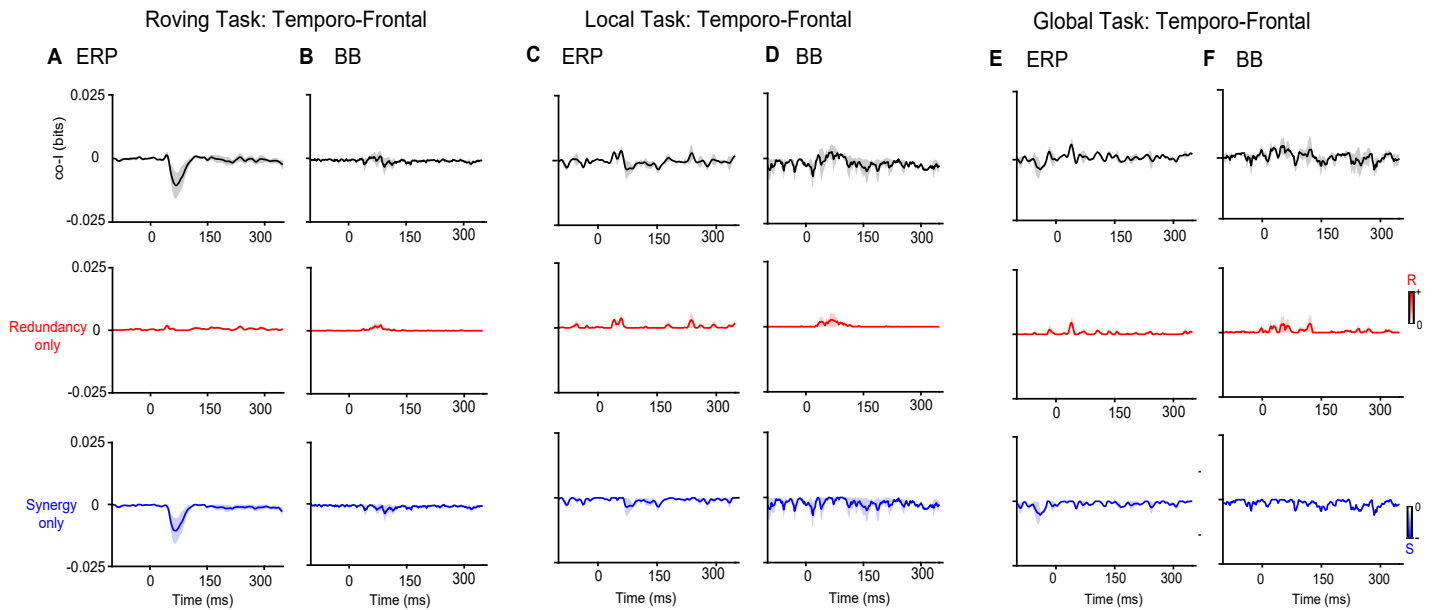
Figure 6: Spatial synergy and redundancy between auditory and frontal electrodes. (A) Roving task (Kr, Go, Fr): Co-Information between auditory and temporal electrodes in the ERP signal. **B**) Roving task (Kr, Go, Fr): Co-Information between auditory and temporal electrodes in the BB signal. Significant spatial synergy was observed in the ERP signal between temporo-frontal electrodes. (C) Local task (Ji, Nr): Co-Information between auditory and temporal electrodes in the ERP signal. (D) Local task (Ji, Nr): Co-Information between auditory and temporal electrodes in the BB signal. (E) Global task (Ji, Nr): Co-Information between auditory and temporal electrodes in the ERP signal. (F) Global task (Ji, Nr): Co-Information between auditory and temporal electrodes in the BB signal. The average of the corresponding temporo-frontal pairs across the three monkeys is shown for the complete co-I values (grey trace), for positive co-I values (redundancy only; red panel), and for negative co-I values (synergy only; blue panel).

for the Local and Global tasks was observed around time points with maximal MI between auditory and frontal electrodes, but mostly within the BB-signal (Figure 7D; e.g. Local Task BB: red cluster ~50-70 ms after tone presentation, F; e.g., Global Task BB; red cluster ~50-70 ms after tone presentation).

To sum up, we observed widespread patterns of synergy within and between electrodes in the temporal and frontal cortices. The dynamics of the synergistic information were observed across distant time points between cortical regions, usually between early and late time points after stimuli presentation. These results suggest that PE information is integrated between areas at both low and high levels of the cortical hierarchy in a synergistic manner, encoded both in time and space by ERP and BB signals.

DISCUSSION

Interpreting redundant interactions

In this study, we focused on computing temporally-resolved metrics of redundancy and synergy, aiming at investigating the dynamics of the information interdependencies within and between cortical signals. Due to the interplay between temporal and spatial information about prediction error, our dynamical approach revealed a rich repertoire of redundant and synergistic patterns, showing transient and sustained information dynamics. Thus, we showed that information was redundant or synergistic across specific time windows, and emerged within and between brain areas.

Redundant patterns of information were observed mainly at time points close to the diagonal of the co-I chart, both within signals (Figures 3-5) and between signals (Figure 7). The advantage of computing redundancy is that it reveals to which extent local and inter-areal signals represent the same information about the stimuli category on a trial-by-trial basis. Redundant interactions about tone category (i.e., deviant or standard) were observed in the ERP and BB signals and represented the outcome of the shared information across time points (temporal redundancy) and between areas (spatio-temporal redundancy). These observed redundancy patterns raise the question of what is the functional relevance of redundant information for processing PE across the cortex.

A neurobiological interpretation of redundancy is that the neural populations encoding this type of information share a common mechanism (Ince et al., 2017). From the perspective of cortical dynamics, redundancy then could provide cortical interactions with robustness (Luppi et al., 2022; Olivares et al., 2022), as redundant interdependencies convey information that is not exclusive to any single cortical region. Robustness, understood as the ability to tolerate perturbations that might affect network functionality (Luppi et al., 2022), is a desirable characteristic of cortical networks processing predictions to preserve stimuli separability in the presence of highly variable stimuli features, environmental noise, or endogenous sources of noise such as background neural activity. Thus, our results suggest that redundancy quantifies the robustness of the information processing in the cortex, enabling multiple areas to process common information about prediction errors.
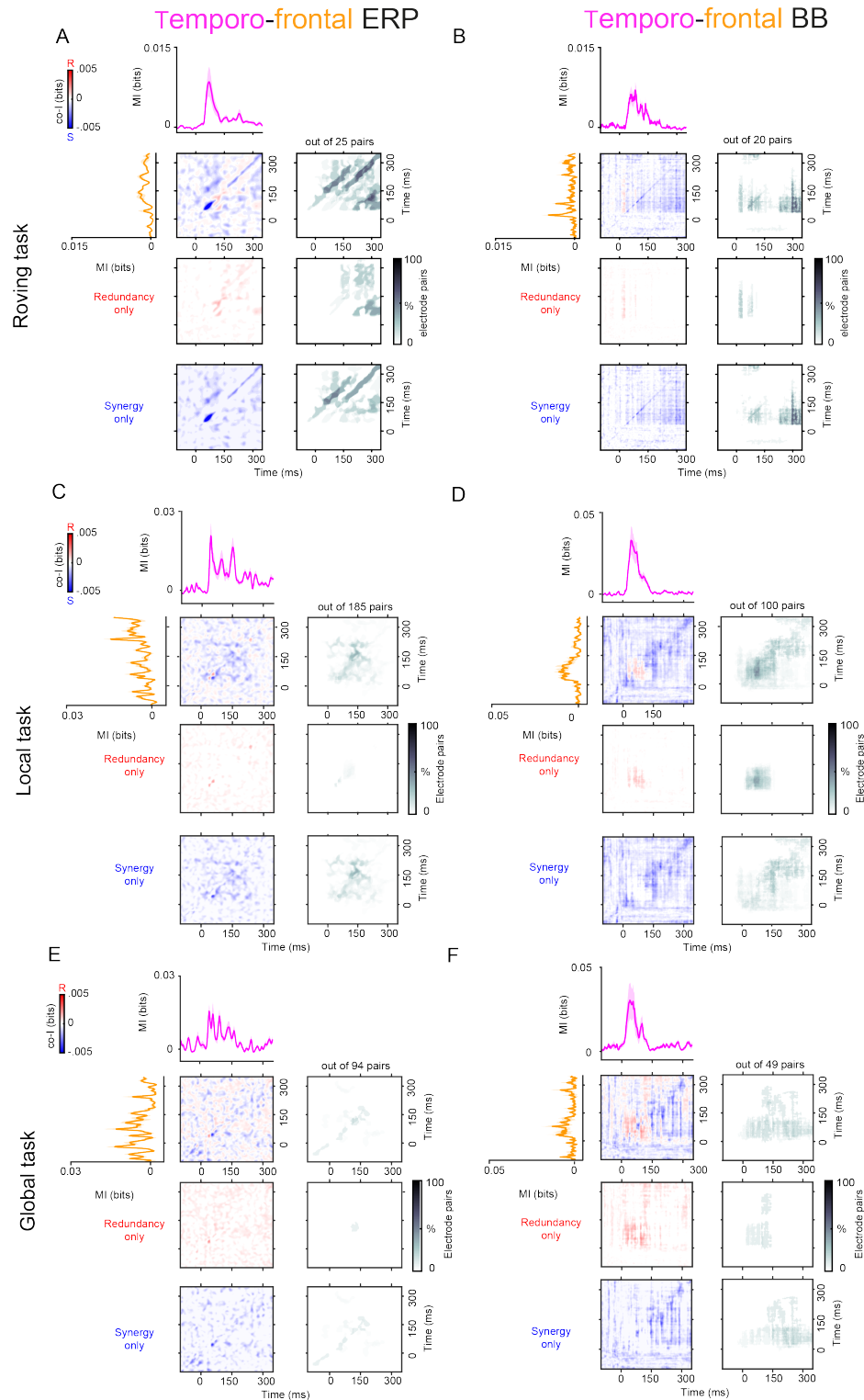
Figure 7: Spatio-temporal synergy and redundancy between auditory and frontal electrodes. Co-information revealed synergistic and redundant spatio-temporal patterns between auditory and frontal electrodes in the ERP (**A**) and BB (**B**) signals for the Roving task (Kr, Go, Fr) and in the ERP (**C,E**) and BB (**D,F**) for the local-global task (Ji, Nr). MI (solid traces) between standard and deviant trials for temporal (pink color) and frontal (orange color) electrodes. Co-I was computed between each pair of electrodes and across time points between -100 to 350 ms after tone presentation. The average of the temporo-frontal pairs across the three monkeys is shown for the complete co-I chart (red and blue panel); for the positive co-I values (redundancy only; red panel); and for the negative co-I values (synergy only; blue panel). The proportion of electrode pairs showing significant co-I differences is shown in the corresponding grey panels. The average co-I charts for the individual monkeys are shown in Figures S3 for the ERP signal, and in Figure S6 for the BB signal for monkeys Fr, Go and (Roving Task). For monkeys Ji and Nr (Local-Global Task), The average co-I charts can be seen in Figures S4, S5 for ERP signal, and Figures S7, S8 for the BB.

9

Interpreting synergistic interactions

A different type of dynamics was observed in the case of the synergistic information across the cortex. While redundant information was observed near the diagonal of the co-I charts, synergistic information was observed mainly off-diagonally, i.e. between early and late times points after tone presentation for both within (Figures 3-5) and between cortical areas (Figure 7).

This indicates that late temporal responses carry information that, in combination with the early one, provides extra information about the identity of the tone (standard or deviant) than when considered in isolation. A neurobiological interpretation of synergy is that the underlying neural populations encode independent but complementary information (Ince et al., 2017).

This raises the question about what is the functional relevance of synergistic information for representing prediction errors. We propose that synergistic interactions could represent a neural marker of biological degeneracy. Degeneracy is the ability of structurally different elements to perform the same function, being a ubiquitous property of many biological systems including neural circuits and networks (Edelman and Gally, 2001). Importantly, degenerative systems are capable of performing different functions (i.e., generalizability and pluripotency) when exposed to changes in contextual circumstances, making them extremely flexible and resilient (Edelman and Gally, 2001).

There is evidence that degeneracy in neural networks may provide various computational benefits, for example, enabling stable computations despite unstable neural dynamics (Driscoll et al., 2017; Druckmann and Chklovskii, 2012) and allowing the central nervous system to filter out unwanted noise (Moreno-Bote et al., 2014). The cortical markers of auditory PE have been observed in auditory subcortical and cortical structures of several species despite the differences in their neuroanatomical structures (Parras et al., 2017; Blenkmann et al., 2019; Canales-Johnson et al., 2021). This suggests that synergistic information is the outcome of distinct neural circuits computing error information in a complementary manner, providing the cortex with a flexible code for representing PE information distributively.

Differences in redundancy and synergy between tasks

The employed tasks all showed distinct patterns of synergistic and redundant dynamics. The Roving task displayed synergistic activity mostly within the ERP signal, while the local deviant in the local-global task displayed temporally distributed synergy within both ERP and BB signals. A possible explanation for this is that the MMN-response for the Roving task could primarily reflect stimulus-specific adaptation at the level of the auditory cortex (O'Reilly, 2021), while the local task shows smaller effects relating to adaptation due to the 20-sequence adaptation period at the start of each testing run (Chao et al., 2018; Jiang et al., 2022). If this is the case, the transient responses to the local/global task

While the local deviant in the local-global task showed highly distributed synergistic activity across brain areas and for both monkeys, the patterns observed for the global deviant were more monkey-dependent. Strong effects were observed within

signals (ERP/BB) and between brain areas (temporal/frontal) for monkey Ji, but monkey Nr exhibited minimal effects within and between all cortical regions (See Figure S2). A speculative explanation for the lack of an effect could be attention-dependent processing for the global deviants: it might be that while processing of local auditory oddball is likely automatic, spotting global deviants requires attentional resources (Chennu et al., 2013; Bekinschtein et al., 2009). In this case, the lack of effects in Nr could be simply explained by a lack of interest in the experimental stimuli.

Regardless of the differences between the conditions, and in line with our interpretation of synergy, i.e., that it captures underlying neuronal populations encoding complementary information, these results indicate that during all three tasks information about stimulus unpredictability is processed in a spatially and temporally distributed fashion across cortical areas.

Distributed processing across cortical areas: Implications for predictive coding theories

Our results show that transient signals (i.e. ERP and BB) encode information about prediction errors and that this information can be synergistic or redundant to reflect how the predictive processing of auditory tones is distributed across the brain. Distinct patterns of synergy within and between brain areas emerge at simultaneous time points for all of the tasks, suggesting a distributive processing of information about unexpected stimuli performed by distinct cortical circuits. This notion can have ramifications for predictive processing accounts. For example, the finding that synergistic information about PE can emerge within signals in the initial stages of the auditory hierarchy (A1), and that parallel clusters of synergistic processing emerge across the brain areas, suggests a more distributed form of computation than postulated by Hierarchical Predictive Coding (HPC) (Chao et al., 2018; Jiang et al., 2022). HPC postulates that PE information should be integrated into successive stages of the hierarchy, from sensory areas (A1) to higher-order areas (frontal cortex). This processing sequence is accompanied by gradual increases in the spatio-temporal processing and complexity of stimuli features. Our findings suggest the alternative view, in line with a more distributed view of brain processing (Steinmetz et al., 2019; Parras et al., 2017; Voitov and Mrsic-Flogel, 2022). Rather than a hierarchy of prediction error processing, we propose that PE information can be encoded in parallel across different temporal scales, which is possibly implemented by recurrent neural circuits across the cortical hierarchy (Vinck et al., 2022).

Conclusion

Inter-areal interactions are traditionally studied using connectivity metrics derived from the spectral decomposition of signals (Vinck et al., 2023). Here we have shown that by characterizing the information content of signals rather than their spectral profile, we can unravel distributed patterns across the cortex encoding complementary information about PE. Thus, our results support the view that distributed representations of prediction error signals across the cortical hierarchy are encoded by synergistic information.

10

Authorship contributions

METHODS

Data acquisition

This study used ECoG recordings from five adult male common marmosets (*Callithrix jacchus*). The details of the datasets for three of the monkeys (Kr, Go and Fr) have been described previously in (Canales-Johnson et al., 2021; Komatsu et al., 2015), and in (Jiang et al., 2022) for two of the monkeys (Ji and Nr).

For marmosets Kr, Go and Fr, (i.e., animals that performed the Roving task) the ECoG recordings were acquired in a passive listening condition while the monkeys were awake. During the recording sessions, the monkeys Go and Kr sat on a primate chair in a dimly lit room, while monkey Fr was held in a drawstring pouch, which was stabilized in a dark room. Every session lasted for about 15 minutes of which the first 3 minutes of data were used for various standard stimuli and the remaining 12 minutes of data acquisition were dedicated to the Roving oddball sequences. For the data analysis, we acquired a total of three sessions for monkey Fr, which resulted in 720 (240 × 3) standard and deviant trials, and six sessions for monkeys Go and Kr, resulting in 1440 (240 × 6) standard and deviant trials. For the recordings, a multi-electrode data acquisition system was used (Cerebus Blackrock Microsystems, Salt Lake City, UT, USA) with a band-pass filter of 0.3–500 Hz and then digitized at 1 kHz. In the signal pre-processing, those signals were re-referenced using an average reference montage, and high-pass filtered above 0.5 Hz, using a 6th-order Butterworth filter.

The recording was done with chronically implanted, customized multielectrode ECoG electrode arrays (Cir-Tech Inc., Japan). Before implantation with the ECoG electrode arrays, the monkeys were anesthetized and further suffering was minimized. All electrodes were implanted in epidural space; 28 in the left hemisphere and an additional 4 in the frontal cortex of the right hemisphere of monkey Fr, 64 in the right hemisphere of monkey Go, and 64 in the right hemisphere of monkey Kr. In the 32-electrode array, each electrode contact was 1 mm in diameter and had an inter-electrode distance of 2.5 - 5.0 mm (Komatsu et al., 2015). In the 64-electrode array, each electrode contact was 0.6 mm in diameter and had an inter-electrode distance of 1.4 mm in a bipolar pair (Komatsu et al., 2019). The electrode arrays covered the temporal, parietal, frontal, and occipital lobes.

For marmosets Ji and Nr, (i.e., the animals that performed the local-global task) the EcoG recordings were also acquired in a passive listening condition while the monkeys were fully awake. The monkeys were seated in sphinx position with their head fixed in a sound-attenuated and electrically shielded room. The recording was done with chronically implanted, multielectrode (96) ECoG electrode arrays (Cir-Tech Inc., Japan). For data analysis, electrodes in temporal and frontal cortices of the marmosets were used. This was done due to the public availability of the data from these electrodes (Jiang et al., 2022). Monkey Ji had a total of 27 electrodes (16 temporal, 11 frontal), and monkey Nr had a total of 39 electrodes (25 temporal, 14 frontal). The data was recorded with a Grapevine NIP system (Ripple Neuro, Salt Lake City, UT) with a sampling rate of 1khz.

All surgical and experimental procedures were performed in accordance with the National Institutes of Health Guidelines for the Care and Use of Laboratory Animals and approved by the RIKEN Ethical Committee (No. H26-2-202, for monkeys Kr, Go and Fr and No. W2020-2-008(2) for monkeys Ji and Nr). The locations of the implanted electrodes of each monkey are found in Figure 2.

Experimental tasks

For the Roving task, monkeys Kr, Go and Fr were subjected to a Roving oddball paradigm (Canales-Johnson et al., 2021). Trains of 3, 5, or 11 repetitive single-tones of twenty different frequencies (250-6727 Hz with intervals of 1/4 octave) were presented in a pseudo-random order. Within each tone train the presented tones had the same frequency, but between tone trains the frequency was different. As the tone trains followed each other continuously, the first tone of a train was considered an unexpected deviant tone, because the preceding tones were of a different frequency, while the expected standard tone was defined as the final tone in a train because the preceding tones were of the same frequency (Figure 1A). The presented tones were pure sinusoidal tones that lasted for 64 ms (7 ms rise/fall) and the time between stimulus onsets was 503 ms. Stimulus presentation was controlled by MATLAB (MathWorks Inc., Natick, MA, USA) using the Psychophysics Toolbox extensions (Brainard and Vision, 1997). Two audio speakers (Fostex, Japan) were used to present the tones with an average intensity of 60 dB SPL around the animal's ear.

For the local/global task, monkeys Ji and Nr were subjected to a standard local/global auditory oddball paradigm (Jiang et al., 2022). The monkeys heard tone trains with either a local regularity (five identical tones played in a sequence; xxxxx) or global regularity (five tones, the first four of which were identical, and where the fifth was of a different frequency; xxxxY). To create a local deviant, the last tone of the local tone train (xxxxx) was sometimes played at a different frequency as the earlier tones in the train (local deviant; xxxxY). To create a global deviant, the last tone of the global tone train (xxxxY) was sometimes played with the same frequency as the earlier tones in the train (global deviant; xxxxx). The frequencies for the tones x or Y were either 707 or 4000hz. The presented tones were pure sinusoidal tones that lasted for 50ms with an intertone interval of 150ms, and they were presented to the monkeys bilaterally with two speakers (Fostex, Japan) from the distance of approximately 20cm from the head with the average intensity of 70 DB.

Each testing period started with a 14 second resting phase, which was followed by a habitation period during which the specified standard (local or global) was presented 20 times to ensure that the monkey learns the regularity of the tone trains. For a testing run, three blocks of 25 tone trains were played, with a 14s resting phase in between. Out of the 25 trials, 20 (80 percent) were of the specified standard (local or global) and five (20 percent) were deviants. For the global deviants, more than one local standard was always played after to ensure global consistency. Each run lasted for 6 minutes and 46 seconds, and

12

each session consisted of 3-4 local standard and 3-4 global standard runs, depending on the marmoset's performance during the day. The order of the tasks was randomised, and the frequencies for tones x and Y were balanced. For the purposes of the analysis, the number of trials for standard and deviant trials had to be equal. This resulted in 330 (local deviant) and 243 (global deviant) trials for Monkey Ji, and 251 (local deviant) and 212 (global deviant) for Monkey Nr.

ERP and BB analyses

For further analysis, the raw ECoG voltage responses have been transformed into ERP and BB as described in Canales-Johnson et al. (2021). In brief, common average referencing was used to re-reference the ECoG recordings across all electrodes, and the data was downsampled to 500hz. For obtaining ERPs, a low-pass filter of 1-40 Hz was applied for the ERP analysis. Standard and deviant tones were categorized as described before. Epochs of -100 ms to 350 ms around the onset of the tones were taken, and a baseline correction was applied by subtracting the mean voltage during the 100 ms period before the stimulus onset from the total epoch.

The MMN signal was determined by subtracting the deviant ERP from the standard ERP.

In order to obtain the BB, spectral decoupling of the raw ECoG was carried out (Canales-Johnson et al., 2021; Miller, 2019). To extract the course of broadband spectral activity, the spectral decoupling of the raw ECoG signal was carried out. As for the ERP analysis, common average referencing was used to re-reference the ECoG potentials of all the electrodes. Epochs of -100 ms to 350 ms around the onset of the tones were used to calculate discrete samples of power spectral density (PSD). Trials from both conditions were grouped together and individual PSDs were normalized with an element-wise division by the average power at each frequency, and the obtained values were log-transformed. In order to identify components of stimulus-related changes in the PSD, a principal component method is applied. This consists of calculating the covariance matrix between the frequencies. The eigenvectors of this decomposition are called Principal Spectral Components (PSCs), and reveal distinct components of neural processing, hence enabling us to identify stimulus-related changes in the PSD. Afterward, the time series were z-scored per trial to get intuitive units, then exponentiated and subtracted by 1. Finally, a baseline correction was performed by subtracting the mean value of the pre-stimulus period of -100 to 0 ms.

Both for the ERP and BB signals some electrodes were excluded from further analysis. This was done because the signal was absent or clearly erroneous. Electrode 18 in Fr was excluded from the ERP analysis, while electrodes 18 in Fr, 30, 44, 45 in Go, and 30 in Kr were excluded from the BB analysis.

Mutual Information analyses

In order to quantify the MI between the stimulus class and the ECoG signal (both ERP and BB), the GCMI toolbox (Gaussian Copula Mutual Information) (Ince et al., 2017) was used. This toolbox calculates the MI based on the Gaussian copula the raw ERP or BB data transforms to. The approach combined a permutation test with 1000 permutations together with a method of maximum statistics in order to correct for multiple comparisons. Using all available trials, the signal at every time point was permuted 1000 times for each electrode, randomly assigning the stimulus class labels each time. The maximum value at each time point was taken, and the 95th percentile of this value was used as the threshold for significance. This method corrects for multiple comparisons and provides a Family-Wise Error Rate (FWER) of 0.05. Electrodes with significant mutual information between standard and deviant trials were selected as electrodes of interest, and the co-information between them was estimated for the ERP and broadband signals separately.

Co-information analyses

We quantified co-Information (co-I) within signals (single electrodes) and between signals (between pairs of electrodes) using the GCMI toolbox (Ince et al., 2017). The co-I was calculated by comparing signals on trial by trial basis. This resulted in a quantification of the information content, redundant or synergistic, between the two signals. The co-information (co-I) was calculated in the following way:

$$coI(X; Y; S) = I(X; S) + I(Y; S) - I(X, Y; S)$$

For each time point, $I(X; S)$ corresponds to the mutual information (MI) between the signal at recording site X and stimuli class S. $I(Y; S)$ corresponds to the MI between the signal at recording site Y and stimuli class S. Finally, $I(X, Y; S)$ corresponds to the MI between stimuli class S combining signals from recording sites X and Y.

For each neural marker of auditory PE (i.e., ERP and BB), co-information was computed for each pair of tones (standard and deviants) within recordings sites in A1 and frontal regions (Figures 3-5 and Figures S1-S2), and between A1 and frontal regions (Figures 6, 7 and Figures S3-S8,). Positive co-information shows that signals between recording sites contain redundant, or overlapping, information about the stimuli. Negative co-information corresponds to the synergy between the two variables: the information when considering the two variables jointly is larger than considering the variables separately.

Figure 1C shows a schematic representation of co-I between two signals. It shows the independent information that response 1 and response 2 (both in white) contain. If there is an overlap in the information that is being represented by the two signals, there is a redundancy (red color) in the information that the two responses contain. If the two signals considered together contain more information than could be expected based on the information present in the individual signals, there is synergy (blue color).

Statistical analyses of co-I charts were performed by using a permutation test with 1000 permutations and using the same maximum statistics method described for the MI analyses, resulting in an FWER of 0.05.
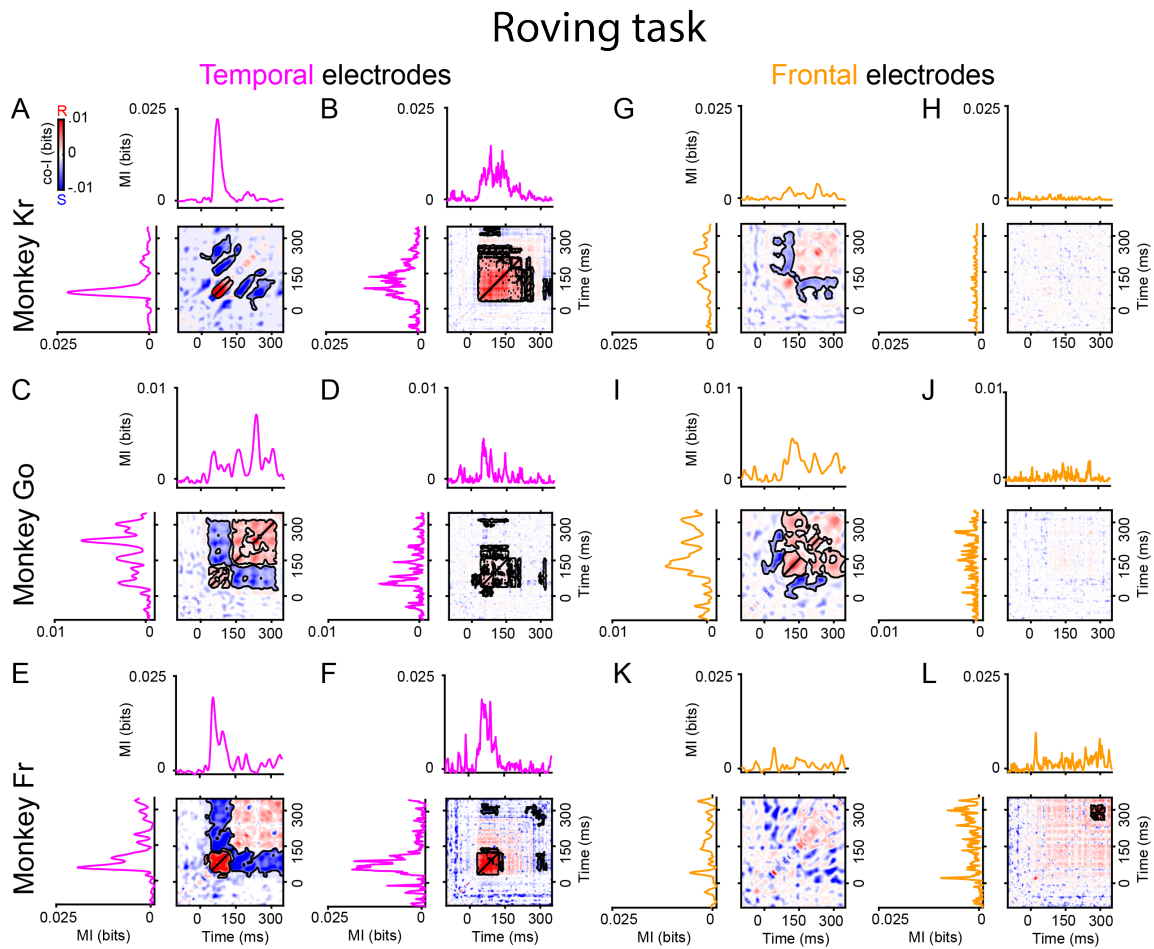
Figure S1: Synergy and redundancy within ERP and within BB signals in temporal and frontal electrodes with the highest MI for the roving task for monkeys Kr, Go and Fr. Co-information within auditory (**A, C, E**), and frontal (**G, I, K**) electrodes in the ERP signal. Co-information within auditory (**B, D, F**), and frontal (**H, J, L**) electrodes in the BB signal. MI (solid traces) between standard and deviant trials for temporal (pink color) and frontal (orange color) electrodes. Co-I was computed between each pair of electrodes and across time points between -100 to 350 ms after tone presentation. Significant temporal clusters after a permutation test (see Methods) are depicted in black contours.
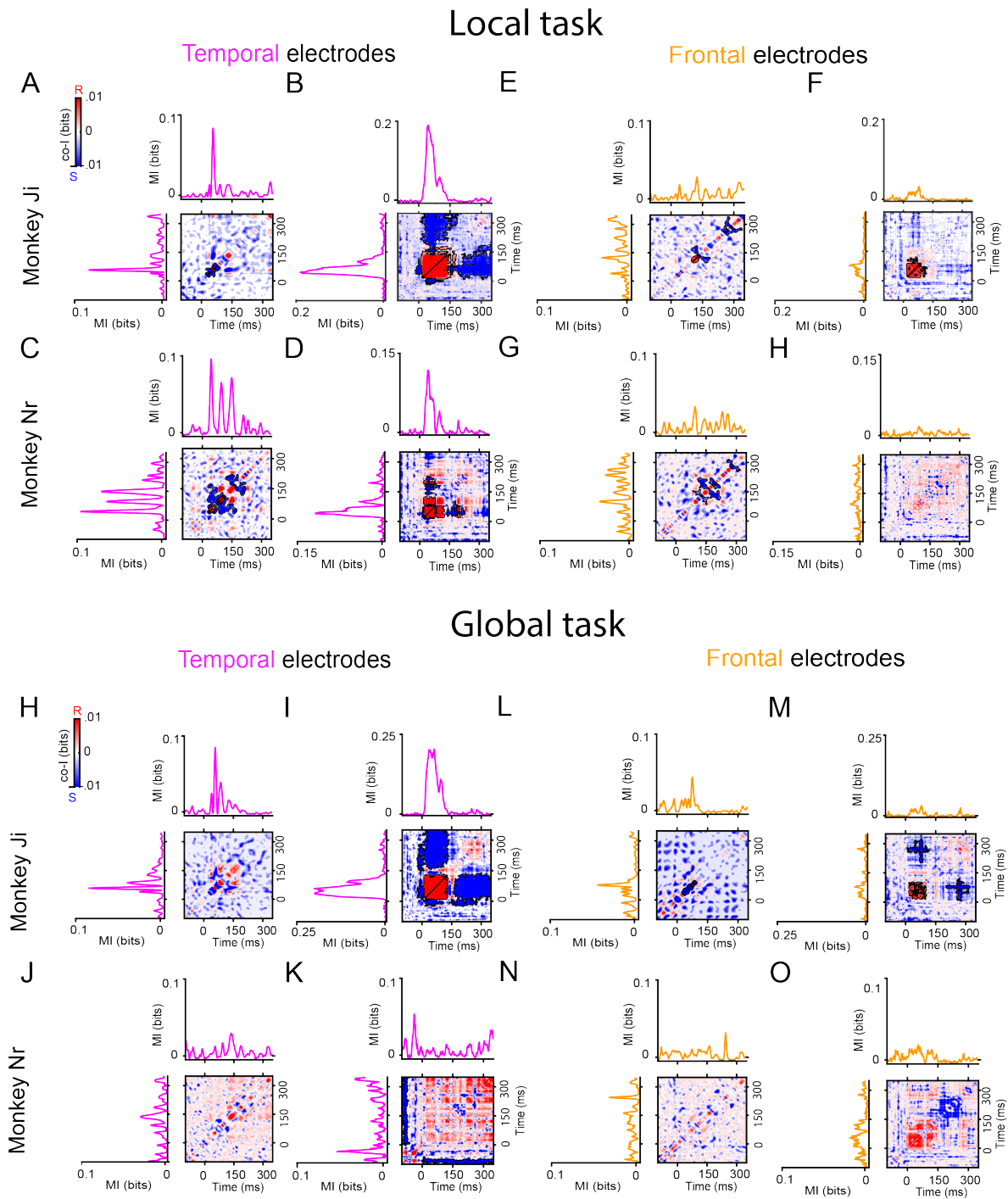
Figure S2: Synergy and redundancy within ERP and within BB signals in temporal and frontal electrodes with the highest MI for the local and global deviants of the local-global task Co-information within auditory (**A, C**), and frontal (**E,G**) electrodes in the ERP signal for the local task. Co-information within auditory (**B,D**), and frontal (**F,H**) electrodes in the BB signal for the local task. Co-information within auditory (**H, J**), and frontal (**L,N**) electrodes in the ERP signal for the global task. Co-information within auditory (**I,K**), and frontal (**M,O**) electrodes in the BB signal for the global task. MI (solid traces) between standard and deviant trials for temporal (pink color) and frontal (orange color) electrodes. Co-I was computed between each pair of electrodes and across time points between -100 to 350 ms after tone presentation. Significant temporal clusters after a permutation test (see Methods) are depicted in black contours.
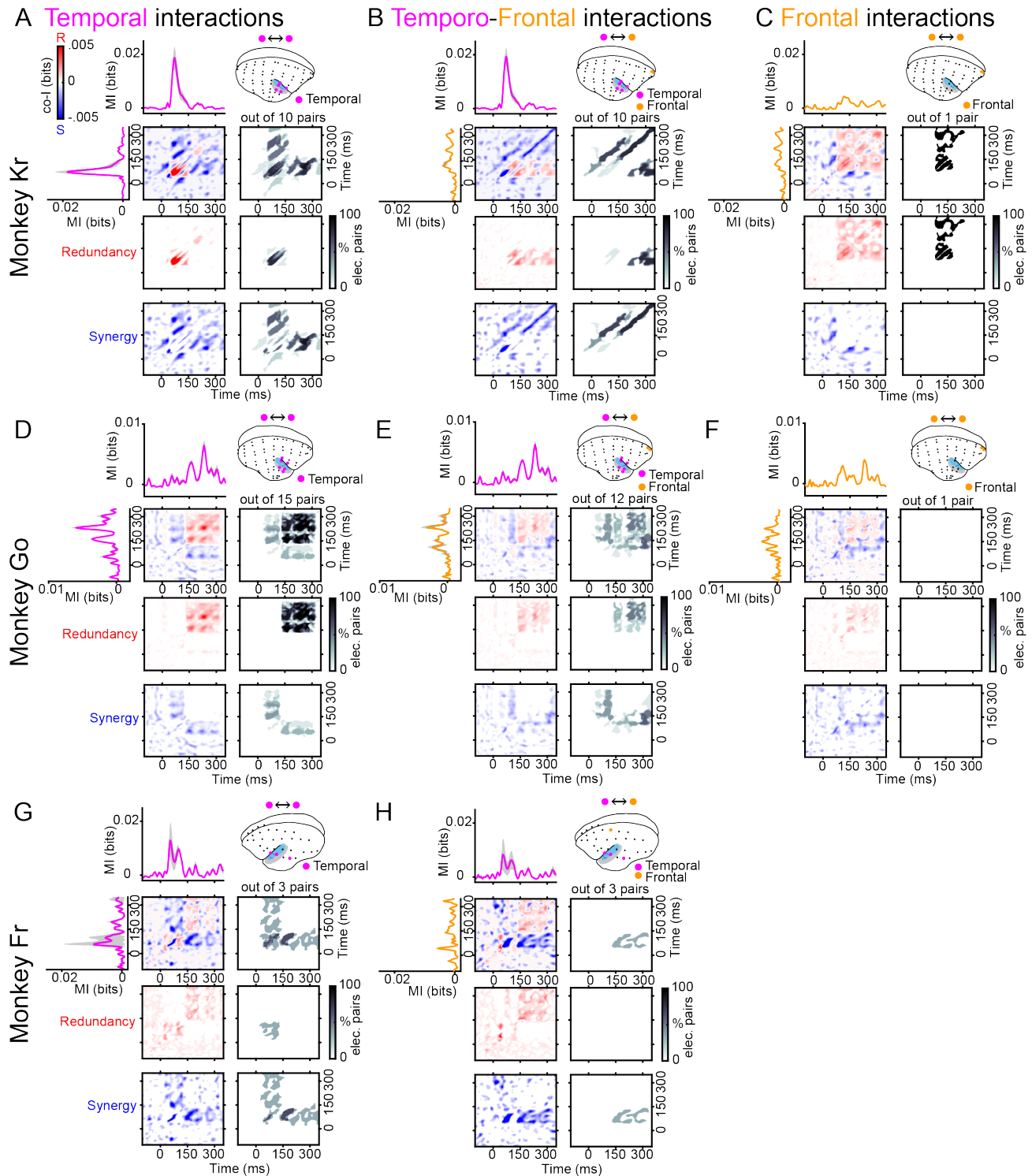
15

Figure S3: Synergy and redundancy between ERP signals and across cortical areas in marmosets Kr, Go and Fr. Co-information revealed synergistic and redundant PE patterns across temporal (**A, D, G**), temporo-frontal (**B, E, H**), and frontal (**C, F**) electrodes. MI (solid traces) between standard and deviant trials for temporal (pink color) and frontal (orange color) electrodes. Co-I was computed between each pair of electrodes and across time points between -100 to 350 ms after tone presentation. The average of the corresponding electrode pairs per (i.e. temporal, temporo-frontal, and frontal) is shown for the complete co-I values (red and blue panel), for positive co-I values (redundancy only; red panel), and negative co-I values (synergy only; blue panel).
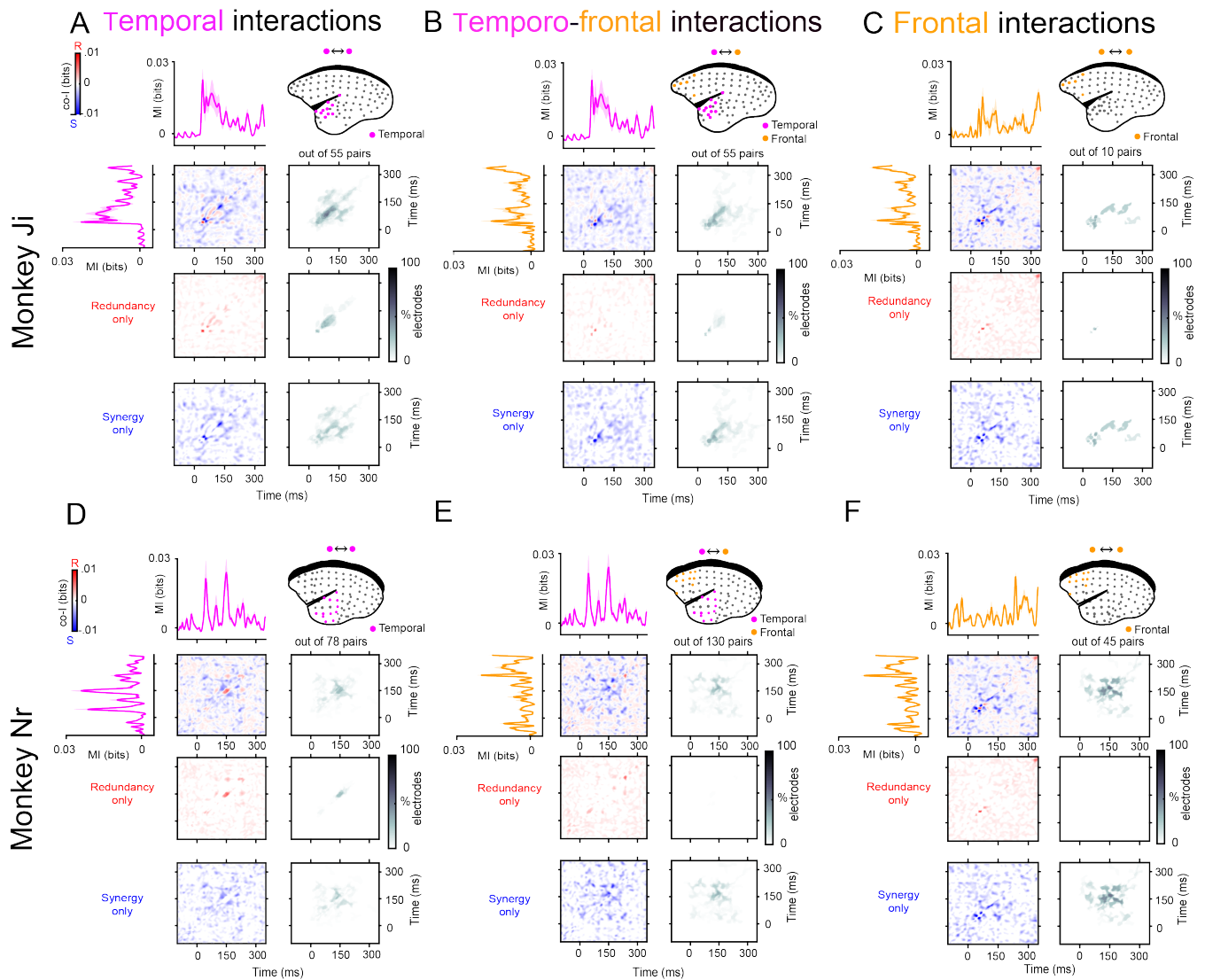
Figure S4: Synergy and redundancy between ERP signals and across cortical areas for marmosets Ji and Nr for the local deviant of the Local-Global task. Co-information revealed synergistic and redundant PE patterns across temporal (**A, D**), temporo-frontal (**B, E**), and frontal (**C, F**) electrodes. MI (solid traces) between standard and deviant trials for temporal (pink color) and frontal (orange color) electrodes. Co-I was computed between each pair of electrodes and across time points between -100 to 350 ms after tone presentation. The average of the corresponding electrode pairs per (i.e. temporal, temporo-frontal, and frontal) is shown for the complete co-I values (red and blue panel), for positive co-I values (redundancy only; red panel), and negative co-I values (synergy only; blue panel).
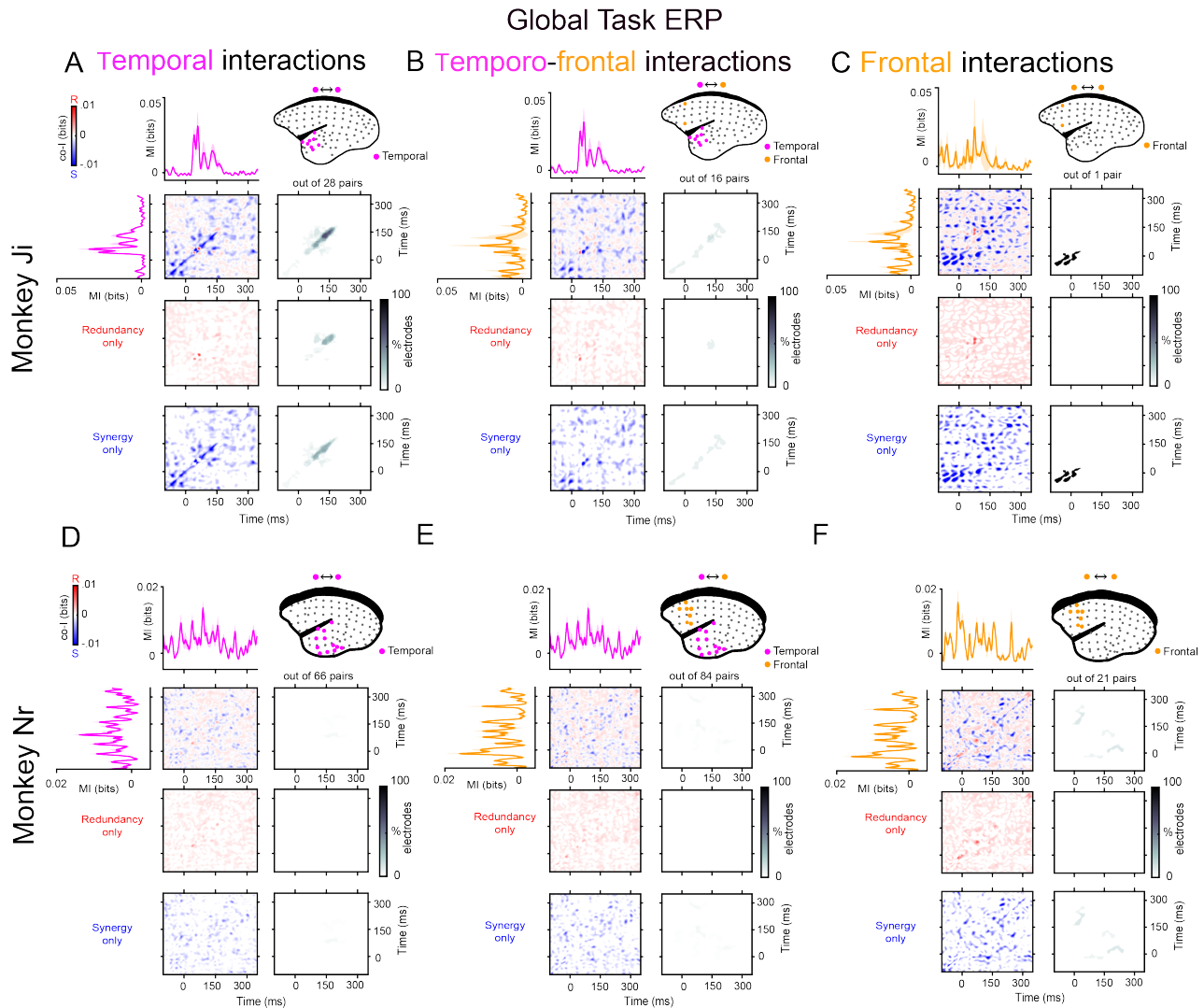
Figure S5: Synergy and redundancy between ERP signals and across cortical areas for marmosets Ji and Nr for the Global deviant of the Local-Global task. Co-information revealed synergistic and redundant PE patterns across temporal **(A, D)**, temporo-frontal **(B, E)**, and frontal **(C, F)** electrodes mostly for marmoset Ji, while Nr only showed relatively weak synergetic patterns between frontal electrodes. MI (solid traces) between standard and deviant trials for temporal (pink color) and frontal (orange color) electrodes. Co-I was computed between each pair of electrodes and across time points between -100 to 350 ms after tone presentation. The average of the corresponding electrode pairs per (i.e. temporal, temporo-frontal, and frontal) is shown for the complete co-I values (red and blue panel), for positive co-I values (redundancy only; red panel), and for negative co-I values (synergy only; blue panel).
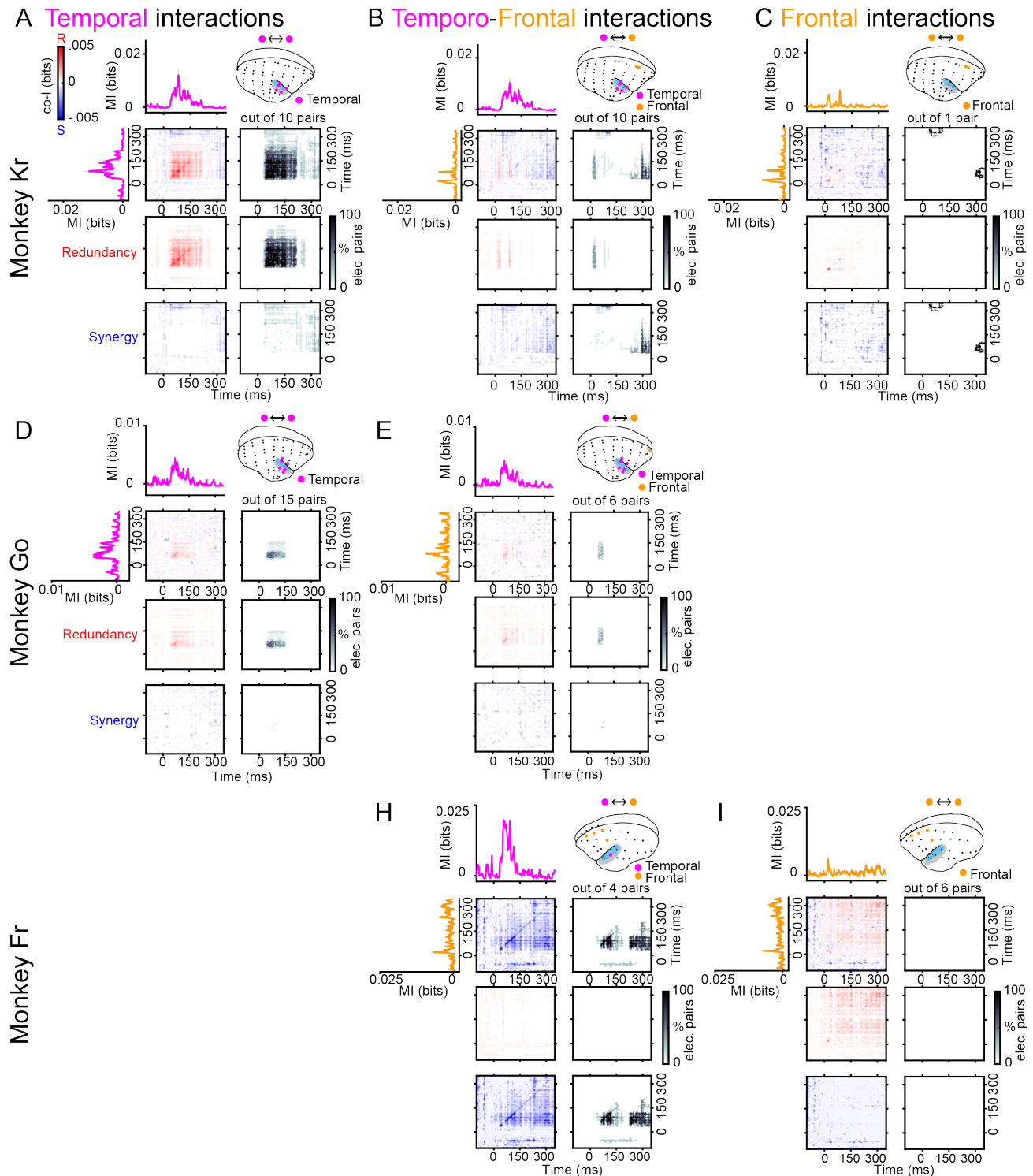
Figure S6: Synergy and redundancy between BB signals and across cortical areas in marmosets Kr, Go and Fr in the Roving task. Co-information revealed synergistic and redundant PE patterns across temporal (**A, D**), temporo-frontal (**B, E, H**), and frontal (**C, I**) electrodes. MI (solid traces) between standard and deviant trials for temporal (pink color) and frontal (orange color) electrodes. Co-I was computed between each pair of electrodes and across time points between -100 to 350 ms after tone presentation. The average of the corresponding electrode pairs per (i.e. temporal, temporo-frontal, and frontal) is shown for the complete co-I values (red and blue panel), for positive co-I values (redundancy only; red panel), and negative co-I values (synergy only; blue panel).
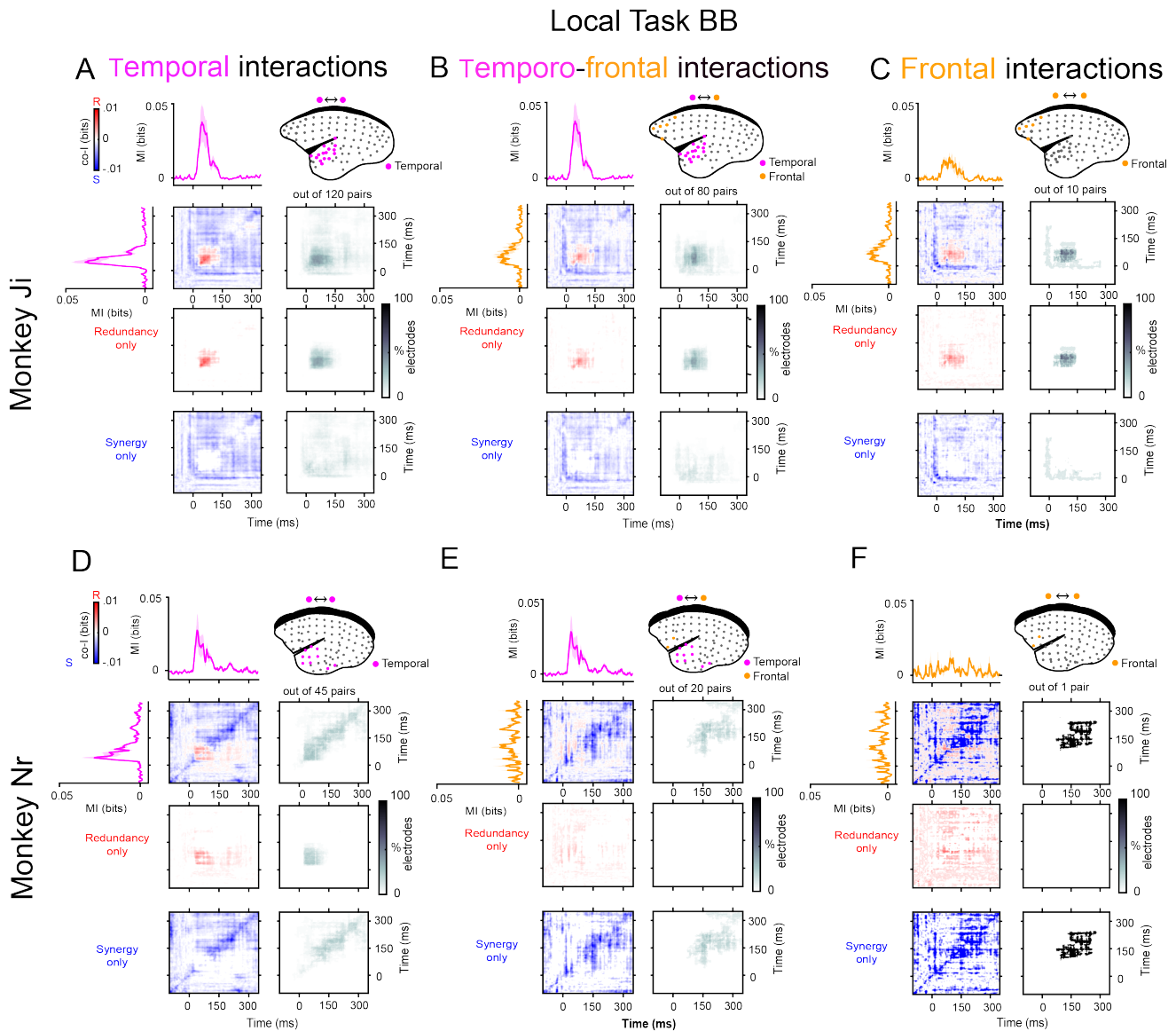
Figure S7: Synergy and redundancy between BB signals and across cortical areas for marmosets Ji and Nr for the local deviant of the Local-Global task. Co-information revealed synergistic and redundant PE patterns across temporal (**A, D**), temporo-frontal (**B, E**), and frontal (**C, F**) electrodes. MI (solid traces) between standard and deviant trials for temporal (pink color) and frontal (orange color) electrodes. Co-I was computed between each pair of electrodes and across time points between -100 to 350 ms after tone presentation. The average of the corresponding electrode pairs per (i.e. temporal, temporo-frontal, and frontal) is shown for the complete co-I values (red and blue panel), for positive co-I values (redundancy only; red panel), and negative co-I values (synergy only; blue panel).
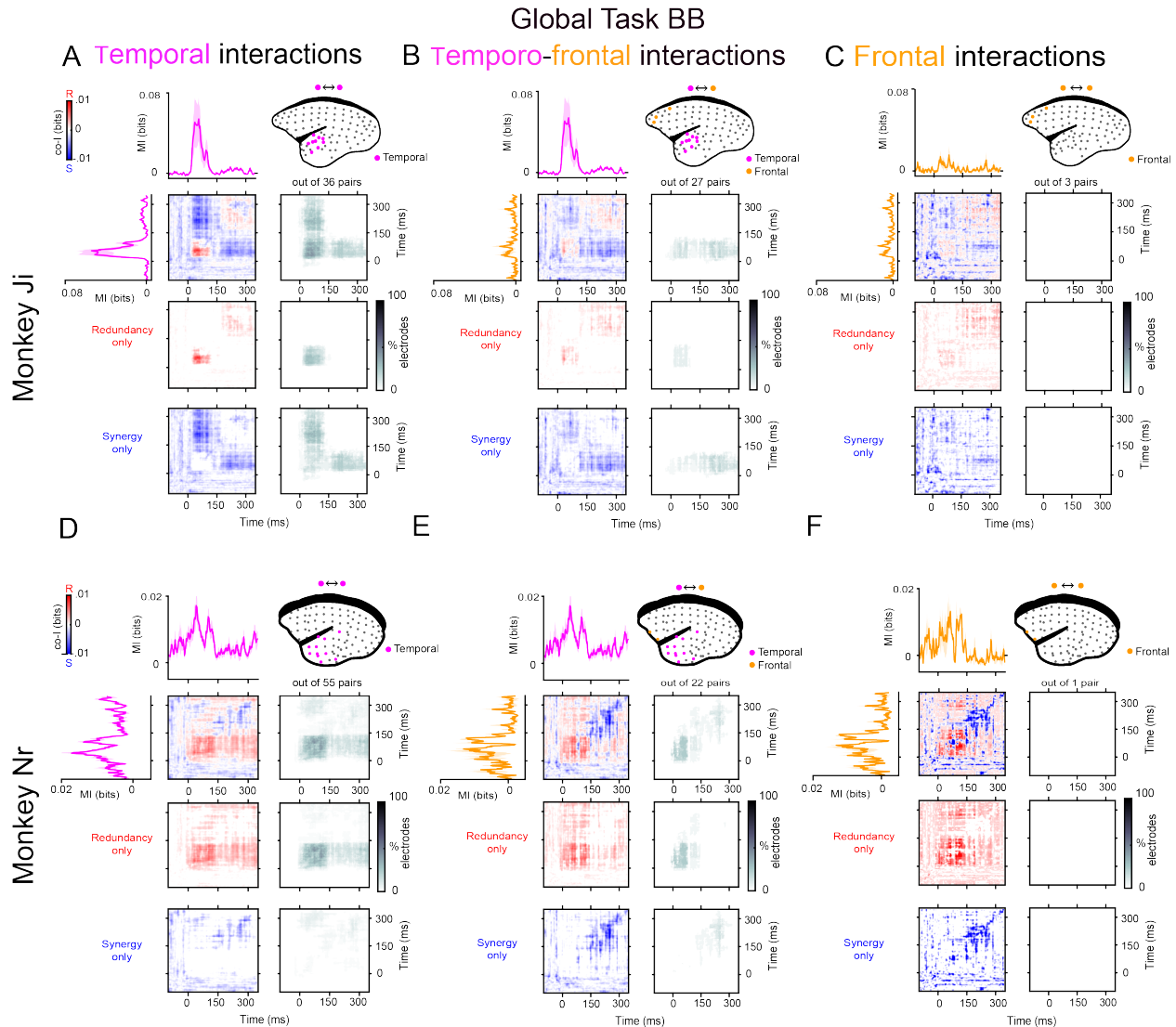
Figure S8: Synergy and redundancy between ERP signals and across cortical areas in marmosets Ji and Nr for the global deviant of the Local-Global task. Co-information revealed synergistic and redundant PE patterns across temporal (**A, D**), temporo-frontal (**B, E**), and frontal (**C, F**) electrodes. MI (solid traces) between standard and deviant trials for temporal (pink color) and frontal (orange color) electrodes. Co-I was computed between each pair of electrodes and across time points between -100 to 350 ms after tone presentation. The average of the corresponding electrode pairs per (i.e. temporal, temporo-frontal, and frontal) is shown for the complete co-I values (red and blue panel), for positive co-I values (redundancy only; red panel), and negative co-I values (synergy only; blue panel).
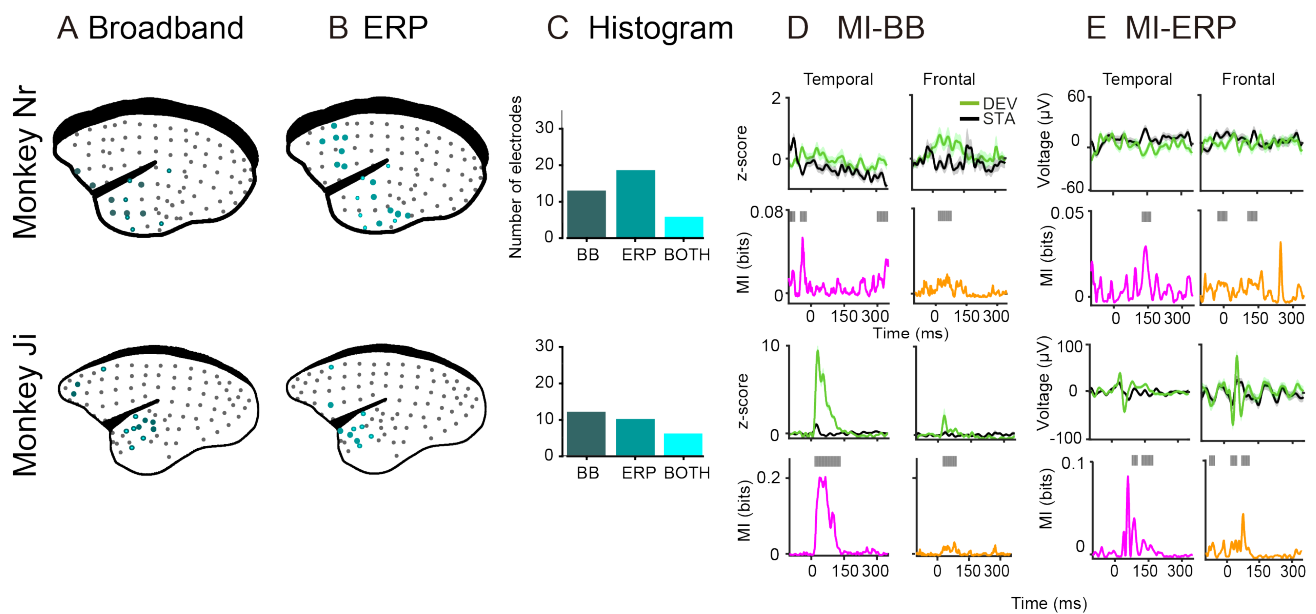
21

Figure S9: Broadband and ERP markers of PE across the monkey brain for monkeys Ji and Nr for the global task. Electrode locations for marmoset Nr (96 electrodes; upper panel) and Ji (96 electrodes; lower panel). Electrodes showing significant PE effect after computing MI between standard and deviant trials for the **(A)** Broadband (dark green circles) and **(B)** ERP (light green circles) markers of auditory prediction error in both monkeys. Electrodes showing significant MI for both markers are depicted in cyan. **(C)** Histogram of electrodes showing significant MI between tones for BB (left), ERP (middle), and both markers (right) for each animal. **(D)** Electrodes with the highest MI in the temporal and frontal cortex showing the BB signal for deviant and standard tones. Deviant tone (green) and standard tone (black), and the corresponding MI values in bits (effect size of the difference) for the temporal (pink trace) and frontal (orange trace) electrodes. Significant time points after a permutation test are shown as grey bars over the MI plots. **(E)** Electrodes with the highest MI in the temporal and frontal cortex showing the ERP signal for deviant and standard tones. Color codes are the same as in **C**.

References

Bekinschtein, T.A., Dehaene, S., Rohaut, B., Tadel, F., Cohen, L., Naccache, L., 2009. Neural signature of the conscious processing of auditory regularities. Proceedings of the National Academy of Sciences 106, 1672–1677.

Bimbard, C., Sit, T.P.H., Lebedeva, A., Reddy, C.B., Harris, K.D., Carandini, M., 2023. Behavioral origin of sound-evoked activity in mouse visual cortex. Nat. Neurosci. .

Blenkmann, A.O., Collavini, S., Lubell, J., Llorens, A., Funderud, I., Ivanovic, J., Larsson, P.G., Meling, T.R., Bekinschtein, T., Kochen, S., Endestad, T., Knight, R.T., Solbakk, A.K., 2019. Auditory deviance detection in the human insula: An intracranial eeg study. Cortex 121, 189–200.

Breakspear, M., 2017. Dynamic models of large-scale brain activity. Nat. Neurosci. 20, 340–352.

Canales-Johnson, A., Teixeira Borges, A.F., Komatsu, M., Fujii, N., Fahrenfort, J.J., Miller, K.J., Noreika, V., 2021. Broadband dynamics rather than frequency-specific rhythms underlie prediction error in the primate auditory cortex 41, 9374–9391.

Chao, Z.C., Takaura, K., Wang, L., Fujii, N., Dehaene, S., 2018. Large-scale cortical networks for hierarchical prediction and prediction error in the primate brain. Neuron 100, 1252–1266.e3.

Chennu, S., Noreika, V., Gueorguiev, D., Blenkmann, A., Kochen, S., Ibánez, A., Owen, A.M., Bekinschtein, T.A., 2013. Expectation and attention in hierarchical auditory prediction. Journal of Neuroscience 33, 11194–11205.

Driscoll, L.N., Pettit, N.L., Minderer, M., Chettih, S.N., Harvey, C.D., 2017. Dynamic reorganization of neuronal activity patterns in parietal cortex. Cell 170, 986–999.e16.

Druckmann, S., Chklovskii, D.B., 2012. Neuronal circuits underlying persistent representations despite time varying activity. Curr. Biol. 22, 2095–2103.

Edelman, G.M., Gally, J.A., 2001. Degeneracy and complexity in biological systems. Proc. Natl. Acad. Sci. U. S. A. 98, 13763–13768.

Giordano, B.L., Ince, R.A.A., Gross, J., Schyns, P.G., Panzeri, S., Kayser, C., 2017. Contributions of local speech encoding and functional connectivity to audio-visual speech perception. eLife 6, e24763.

Ince, R.A., Giordano, B.L., Kayser, C., Rousselet, G.A., Gross, J., Schyns, P.G., 2017. A statistical framework for neuroimaging data analysis based on mutual information estimated via a gaussian copula. Human Brain Mapping 38, 1541–1573.

Jiang, Y., Komatsu, M., Chen, Y., Xie, R., Zhang, K., Xia, Y., Gui, P., Liang, Z., Wang, L., 2022. Constructing the hierarchy of predictive auditory sequences in the marmoset brain. eLife 11, e74653.

Komatsu, M., Kaneko, T., Okano, H., Ichinohe, N., 2019. Chronic implantation of whole-cortical electrocorticographic array in the common marmoset. J. Vis. Exp. .

Komatsu, M., Takaura, K., Fujii, N., 2015. Mismatch negativity in common marmosets: Whole-cortical recordings with multi-channel electrocorticograms. Sci. Rep. 5, 15006.

Lachaux, J.P., Axmacher, N., Mormann, F., Halgren, E., Crone, N.E., 2012. High-frequency neural activity and human cognition: Past, present and possible future of intracranial eeg research. Progress in Neurobiology 98, 279–301. High Frequency Oscillations in Cognition and Epilepsy.

Lohuis, M.N.O., Marchesi, P., Olcese, U., Pennartz, C., 2022. Triple dissociation of visual, auditory and motor processing in primary visual cortex. bioRxiv .

Luppi, A.I., Mediano, P.A.M., Rosas, F.E., Holland, N., Fryer, T.D., O'Brien, J.T., Rowe, J.B., Menon, D.K., Bor, D., Stamatakis, E.A., 2022. A synergistic core for human brain evolution and cognition. Nat. Neurosci. 25, 771–782.

Miller, K.J., 2019. A library of human electrocorticographic data and analyses. Nat. Hum. Behav. 3, 1225–1235.

Moreno-Bote, R., Beck, J., Kanitscheider, I., Pitkow, X., Latham, P., Pouget, A., 2014. Information-limiting correlations. Nat. Neurosci. 17, 1410–1417.

Nigam, S., Pojoga, S., Dragoi, V., 2019. Synergistic coding of visual information in columnar networks. Neuron 104, 402–411.e4.

Olivares, J., Orio, P., Sadílek, V., Schmachtenberg, O., Canales-Johnson, A., 2022. Neural oscillations across olfactory regions encode odorant information in the teleost olfactory system doi:10.1101/2022.04.15.488302.

O'Reilly, J.A., 2021. Roving oddball paradigm elicits sensory gating, frequency sensitivity, and long-latency response in common marmosets. IBRO Neuroscience Reports 11, 128–136.

Panzeri, S., Moroni, M., Safaai, H., Harvey, C.D., 2022. The structures and functions of correlations in neural population codes. Nat. Rev. Neurosci. 23, 551–567.

Park, H., Ince, R.A.A., Schyns, P.G., Thut, G., Gross, J., 2018. Representational interactions during audiovisual speech entrainment: Redundancy in left posterior superior temporal gyrus and synergy in left motor cortex. PLOS Biology 16, 1–26.

Parras, G.G., Nieto-Diego, J., Carbajal, G.V., Valdés-Baizabal, C., Escera, C., Malmierca, M.S., 2017. Neurons along the auditory pathway exhibit a hierarchical organization of prediction error. Nat. Commun. 8, 2148.

Rao, R.P., Ballard, D.H., 1999. Predictive coding in the visual cortex: a functional interpretation of some extra-classical receptive-field effects. Nat. Neurosci. 2, 79–87.

Saleem, A.B., Diamanti, E.M., Fournier, J., Harris, K.D., Carandini, M., 2018. Coherent encoding of subjective spatial position in visual cortex and hippocampus. Nature 562, 124–127.

de Schotten, M.T., Forkel, S.J., 2022. The emergent properties of the connected brain. Science 378, 505–510.

Shenoy, K.V., Kao, J.C., 2021. Measurement, manipulation and modeling of brain-wide neural population dynamics. Nat. Commun. 12, 633.

Steinmetz, N.A., Zatka-Haas, P., Carandini, M., Harris, K.D., 2019. Distributed coding of choice, action and engagement across the mouse brain. Nature 576, 266–273.

Urai, A.E., Doiron, B., Leifer, A.M., Churchland, A.K., 2022. Large-scale neural recordings call for new insights to link brain and behavior. Nat. Neurosci. 25, 11–19.

Varley, T.F., Sporns, O., Schaffelhofer, S., Scherberger, H., Dann, B., 2023. Information-processing dynamics in neural networks of macaque cerebral cortex reflect cognitive state and behavior. Proc. Natl. Acad. Sci. U. S. A. 120, e2207677120.

Vinck, M., Uran, C., Canales-Johnson, A., 2022. The neural dynamics of feedforward and feedback interactions in predictive processing. doi:10.31234/osf.io/n3afb.

Vinck, M., Uran, C., Spyropoulos, G., Onorato, I., Broggini, A.C., Schneider, M., Canales-Johnson, A., 2023. Principles of large-scale neural interactions. Neuron 111, 987–1002.

Voitov, I., Mrsic-Flogel, T.D., 2022. Cortical feedback loops bind distributed representations of working memory. Nature 608, 381–389.